DRAG REDUCTION OF A HULL BY ELECTROLYSIS

Wayne A. Thornton

Naval Academy
Annapolis, Maryland

21 May 1974

UNCLASSIFIED
Security Classification

AD-784 122

DOCUMENT CONTROL DATA - R & D

(Security classification of title, body of abstract and indexing annotation must be entered when the overall report is classified)

1 ORIGINATING ACTIVITY (Corporate author)

U.S. Naval Academy, Annapolis.

2a. REPORT SECURITY CLASSIFICATION

UNCLASSIFIED.

2b. GROUP

3 REPORT TITLE

Drag reduction of a hull by electrolysis.

4 DESCRIPTIVE NOTES (Type of report and inclusive dates)

Research report.

5. AUTHOR(S) (First name, middle initial, last name)

Wayne A. Thornton.

6 REPORT DATE	7a. TOTAL NO. OF PAGES	7b. NO. OF REFS
21 May 1974.	[4] 64 [19]	29.

8a. CONTRACT OR GRANT NO

b. PROJECT NO.

c.

d.

9a. ORIGINATOR'S REPORT NUMBER(S)

U.S. Naval Academy - Trident Scholar project report (U.S.N.A.-TSPR) no. 63.

9b. OTHER REPORT NO(S) (Any other numbers that may be assigned this report)

10 DISTRIBUTION STATEMENT

This document has been approved for public release; its distribution is UNLIMITED.

11. SUPPLEMENTARY NOTES

12. SPONSORING MILITARY ACTIVITY

U.S. Naval Academy, Annapolis.

13. ABSTRACT

This experiment was conducted to study the drag reduction on a hull resulting from injection of gas bubbles into the boundary layer by electrolysis.

The resulting drag reduction on the 18'2" model was found to depend on the towing velocity and the time-rate of gas bubbles produced at the electrodes. The drag reduction obtained on the 18'2" model at a fixed current of 4 amperes was found to vary between 3.2 o/o at the lower towing speeds and 17.5 o/o in the middle of the speed range. With increasing speed, the bubble injection had a diminishing effect. For the maximum drag reduction, the power requirement was 50.4 watts.

Projecting these results to prototype application, it appears that the effect is a function of the wetted surface area of the hull.

The detailed procedures and findings are presented.

"DRAG REDUCTION OF A HULL BY ELECTROLYSIS"

A Trident Scholar Project Report

by

Midshipman Wayne A. Thornton
Class of 1974

U. S. Naval Academy
Annapolis, Maryland

Michael E. McCormick

Dr. M. E. McCormick
Naval Systems Engineering Dept.

Accepted for Trident Scholar Committee

V V Ostapoff

21 May 1974

ABSTRACT

A series of experiments was conducted to study the drag reduction on a hull resulting from injection of gas bubbles into the boundary layer by electrolysis. Preliminary tests were conducted on a 5' displacement hull and the final tests were performed on an 18'2" hull of the same type.

Analysis of the motion of the gas bubbles in the flow around the hull for a range of speeds verified the conclusion reached by McCormick and Bhattacharrya in earlier tests that a large number of electrodes should be placed forward on the hull to insure maximum bubble distribution in the flow. However, to replace bubbles lost in separation banks of electrodes should be located at those points on the hull where separation occurs.

The resulting drag reduction on the 18'2" model was found to depend on the towing velocity and the time-rate of gas bubbles produced at the electrodes.

Furthermore, the power necessary to generate a given current was found to decrease by as much as 42% of the power necessary for static conditions. Hence, the mass flow rate of gas generated is dependent on the mass flow rate of the water past the hull.

The drag reduction obtained on the 18'2" at a fixed

current of 4 amperes was found to vary between 3.2% at the lower towing speeds and 17.5% in the middle of the speed range. With increasing speed, the bubble injection had a diminishing effect. For the maximum drag reduction the power requirement, was 50.4 watts.

Projecting these results to prototype application, it appears that the effect is a function of the wetted surface area of the hull. Due to the fact that seawater is a considerably better conductor than freshwater, the electrolytic cell resistance can almost be neglected if a sufficient number of electrode pairs are connected in parallel. The limiting minimum voltage is equal to the oxidation-reduction potential and over-potential for the reactions involved. Hence the corresponding power requirement for the full-scale hull is 0.39 KW (which corresponds to 0.53HP). It is readily apparent that the input power to achieve a rather significant drag reduction is so small that a considerable fuel savings and extended cruising range can be realized using the technique of drag reduction by electrolysis.

ACKNOWLEDGEMENTS

The author would like to express sincerest appreciateion to the many people who contributed their time, efforts, ideas, and encouragement

Dr. M. E. McCormick, Professer, Naval Systems Engineering Dept., U. S. Naval Academy

Dr. F. I. Davis, Asst. Professor, Mathematics Dept., U. S. Naval Academy

LTjg J. J. Fontanella, Instructor, Physics Dept., U. S. Naval Academy

Dr. W. M. Smedley, Professor, Chemistry Dept., U. S. Naval Academy

Mr. J. W. Enzinger, Technical Support Dept., Division of Engineering and Weapons, U. S. Naval Academy

Mr. S. Enzinger, Technical Support Dept., Division of Engineering and Weapons, U. S. Naval Academy

Mr. E. B. Bosworth, Technical Support Dept., Division of Engineering and Weapons, U. S. Naval Academy

Mr. Bruce Crook, Naval Ship Research and Development Center, Carderock, Md.

Mr. Bob Wise, Naval Ship Research and Development Center, Carderock, Md.

Mr. T. J. Lamb, Engelhard Industries, Newark, N.J.

Mr. E. P. Gilroy, General Electric Co.,Cleveland, Ohio

and also to his roommate, Midshipman T. H. Glesser, without whose assistance this project would have been completed a month earlier.

TABLE OF CONTENTS

I. INTRODUCTION

A. Background

Reduction of the fluid resistance on marine vehicles has long been the dream of naval architects and hydrodynamicists. Several methods have been attempted, including boundary-layer suction, the use of compliant hull surfaces, and injection of polymers and compressed gases into the boundary layer. It has been found that the boundary-layer suction method is not practical because it requires excessive amounts of power, and the use of compliant materials is not feasible for large vessels. An excellent summary of those methods used prior to 1964 is presented in a paper by Lumley (19) and a bibliography of recent publications in the area of vehicle resistance is presented by Lap (15).

The method of drag reduction by injection of particles into the fluid stream adjacent to the surface appears much more promising. Research into this area was first conducted by Nora Blatch in 1906, who studied the drag reduction in turbulent flows of dilute suspensions using aqueous suspensions of sand. In 1946, the "Tom's Effect" was discovered which

concerned the reduction of hydraulic resistance caused by injection of small amounts of polymers, and other non-Newtonian additives into the flow.[1] Most of the efforts in drag reduction research subsequent to 1964 have concentrated on the use of polymers. However there are significant disadvantages to any technique which involves the injection of material through the hull of a vehicle. These methods require large chemical mixing and holding tanks, extensive piping, and hull penetrations that are subject to biological fouling.

In this paper, the results of an experimental study of drag reduction by electrolysis are presented. The experiments were based on the results of two studies conducted by McCormick and Bhattacharrya in 1972-73. (Reference 20) In the first study, a series of tests was conducted on a 3-foot fully submerged body of revolution. A 6-mil diameter copper wire was wound around the body and was connected to a DC voltage source to serve as the cathode for the reaction. The positive terminal of the voltage source was connected to the wall of the stainless steel tank in which the model was towed. Bubbles of hydrogen gas were generated at the cathode

wire and subsequently washed into the flow adjacent to the hull. It was found that the introduction of the gas into the boundary layer significantly reduced the viscous resistance on the body. The magnitude of the drag reduction was found to depend on both the towing speed and the applied electrical current to the electrode.

In the subsequent study the cathode was attached to the hull of a 6'9" model of a World War II vintage destroyer which was also towed in the freshwater tank. The results of this study indicated that the reduction of viscous drag was due to the time-rate of mass of hydrogen produced on the hull-mounted cathode and the condition of the flow within the boundary layer adjacent to the hull.

Although the literature on the microscopic effects [illegible] phenomenon is quite extensive, there is no agreement with regard to physical mechanics. It was formerly assumed that suspended additives suppress the turbulence intensity of the flow thereby causing a reduction in the viscous resistance. However, this theory is unsatisfactory because many experiments have shown the polymer additives have a negligible effect on turbulence energy and in some cases have even

increased the energy.[2] McCormick has proposed that the reduction in drag when bubbles are injected into the fluid stream is due to two different mechanisms, depending on the condition of flow within the boundary layer. If the flow is laminar, the bubbles act as a lubricant as they remain close to, or intact with, the hull. When the flow is turbulent the bubbles initially destroy the laminar sublayer, that region being one of high shear stress. As the bubbles travel into the inner and outer regions of the boundary layer they absorb the turbulent momentum and, in addition, act as a lubricant against the small viscous shear stresses in these regions.[3]

There is great difficulty in developing a quantitative theory to model the effect because of a lack of representative atatistical theory applicable to homogenous and non-homogenous turbulence near a wall. However, Buevich has recently developed a model for drag reduction by injection of particles into turbulent viscous flow which corresponds at least qualitatively with observed effects.

B. Purpose of Study

The purposes of this study were to first analyze the technique of drag reduction by electrolysis in a series

of small model tests in an effort to optimize the configuration of the electrodes on the hull for maximum drag reducing effect and to then test the configuration on a larger scale model. Furthermore, the factors determining the power requirement for generating a specified current were to be analyzed and modelled to provide techniques for further optimizing the design configuration, for predicting power requirements and for projecting the results to prototype application.

II. CONSIDERATIONS IN ELECTROLYSIS OF SEAWATER

A. Chemistry of Electrolysis

In the electrolysis of water, which has made an electrolyte by the addition of some conducting ions, bubbles of hydrogen and oxygen gas are generated in the following reactions:

Cathode (oxidation reaction):

$2H^+ + 2e^- = H_2$ (acidic medium)

$2H_2O + 2e^- = H_2 + 2OH^-$ (alkaline medium)

Anode (reduction reaction):

$AH_2O = O_2 + 4H^+ + 4e^-$ (acidic medium)

$4OH^- = O_2 + 2H_2O + 4e^-$ (alkaline medium)

Most natural waters are alkaline, (with the pH of seawater varying between 7.5 and 8.4) and so it is the latter of each pair of reactions that we are concerned with.

Chlorine, (present in seawater as the chloride ion, in average concentrations of 19 parts per thousand) has a lower overvoltage than oxygen. Hence chlorine evolution will predominate at the anode below a specified current density and is oxidized as follows:

$2Cl^- = Cl_2 + 2e^-$

Above the limiting current density, both oxygen and chlorine will be evolved at the anode.

Of significance also are several other reactions which we can expect in the electrolysis of seawater. Scale deposits will form on the cathode due to the precipitation of calcium, sodium, and magnesium salts, and the production of biproducts of hydrogen chloride, hypochlorite, sodium hypochlorite will occur at the anode. The pertinent reactions are listed below:

Cathode: $Na^{+} + OH^{-} = NaOH$

$$Ca^{+2} + 2OH^{-} = 2Ca(OH)_2$$

$$Mg^{+2} + 2OH^{-} = 2Mg(OH)_2$$

Anode: $H_2O + Cl_2 = HCl(aq) + HOCl(aq)$*

$$2NaOH(aq) + Cl_2 = NaOCl(aq) + h_2O$$

In electroflotation oil separators it has been found that pulsing the voltage to the electrodes or impressing an alternating voltage on the DC volutage will reduce the formation of scale on the electrodes. (reference 22).

*It should be noted that these compunds are poisonous to fouling organisms and will provide anti-fouling for the hull.

B. Bubble Growth and Detachment

Bubble growth and detachment and the size of the bubbles generated in electrolysis has been studied by Coehn and Neumann (2) and Kabanov (14). Their findings indicate that bubble size varies with concentration and pH of the electrolyte, and the current density. In dilute solutions and at high current densities, the bubbles evolved are smaller than in concentrated solutions or low current densities.

The effect of current density can be explained by recalling that a number of forces interact which affect the detachment of a bubble including surface tension and contact angle, hydrostatic lift, hydrostatic pressure, and the electric field at the electrified interface. Hence, as the current density increases, the charge of the electrified interface is increased. The resulting increase in the wettability of the surface causes the contact angle to decrease, which in turn causes a decrease in the force of adherence and in the size of the detached bubble.

Furthermore, in alkaline solutions smaller bubbles separate from the cathode than from the anode, but in acidic electrolytes the reverse is true. Hence, we can

expect that in fresh water (pH slightly greater than 7.2) at high current densities the oxygen and hydrogen bubbles will be of similar size and will create a milky turbidity in the water indicating colloidal or emulsion size (0.001 to 0.1 μm). In seawater, which is more alkaline, at the same current density we can expect that the hydrogen bubble size will still be in the colloidal range, but the oxygen bubbles will be somewhat larger.

Epstein and Plesset (2), obtained the following relation for computing the radii of gas bubbles generated by electrolysis:

$$R = 2\left(\frac{3}{\pi}\right)^{0.5} \sqrt{\frac{D}{\rho_g}}\ \Delta C \sqrt{t} \qquad (2.1)$$

R = radius of bubble

D = mass diffusirity of dissolved gas in liquid

ρ_g = density of gas

ΔC = gas concentration differential between electrode

t = time

For a more detailed analysis of bubble growth see references (2) and (14).

C. Effective Bubble Production

The total quantity of gas produced is a function of the current passing through the electrochemical circuit, and can be computed using Farraday's law.

$$\dot{m}_G = \frac{MI}{ZF} \qquad (2.2)$$

$\dot{m}_G$ = time rate of gas production (grams/sec)

M = moleular weight of gas (grams/mole)

I = current (amperes)

Z = Valence number

F = Farraday's constant (F = 96,493 coulombs/mole)

Since hydrogen, chlorine and oxygen gases are soluble in water, one must take this factor into account when computing effective bubble production. The solubility is a function of water temperature, salinity, biological activity, current and wave action, and depth (pressure).

A portion of solubility data tabulated in Sverdrup (28) for oxygen (at one atmosphere pressure) in seawater of various chlorinities and temperatures is reproduced below.

SATURATION VALUES OF OXYGEN IN SEAWATER (Ml/l)

Temperature (°C) \ Chlorinity °/oo	15	16	17
0	8.55	8.43	8.43
5	7.56	7.46	7.36
10	6.77	6.69	6.60
15	6.14	6.07	6.00
20	6.53	5.56	5.50
25	5.17	5.12	5.06

	18	19	20
0	8.20	8.08	7.97
5	7.26	7.16	7.07
10	6.52	6.44	6.35
15	5.93	5.86	5.79
20	5.44	5.38	5.31
25	5.00	4.95	4.86

For the range of values of chlorinities and temperatures given, it can be seen that the saturation value is approximately a linear decreasing function of chlorinity.

Glasstone and Lewis (12) give the equation relating temperature and in the solubility of a gas as

$$\log \frac{\alpha_2}{\alpha_1} = \frac{\Delta H}{2.303R} \frac{(T_2 - T_1)}{(T_1 - T_2)} \qquad (2.3)$$

ΔH = change of enthalpy accompanying solution of 1 mole of gas.

α_1, α_2 = Absorption coefficients (ml/l)

T_2 = temperature

T_1 = reference temperature

R = Gas constant

The influence of pressure on the solubility of a gas was expressed by W. Henry. His conclusions, generally known as Henry's Law, can be stated in equation form as

$W = Kp$ W - mass of gas dissolved per unit volume of solvent

p = equilabrum pressure

K - proportionality constant

Hence solubility is a linear function of pressure. In the range of temperatures experienced in seawater, and for a limited range of depths, most gases obey Henry's Law. However, chlorine reacts chemically with seawater and use of Henry's Law produces inaccurate results when considering its total solubility.

The effective bubble production can be estimated by computing the theoritical gas production per unit length of electrode using Farraday's law. For varying ship's speed, the mass flow rate of water past an electrode of unit length can be computed. To assume "worst case" conditions in order to obtain a conservative estimate, one can assume a chlorinity value of 36 ‰ and temperature of 15°C (the average temperature

at 60°N Latitude).

It must be recalled that Henry's Law is only valid for a specified range of pressures and one must refer to tabulated data to obtain accurate predictions. For a surface ship, the solubility data for a pressure of one atmosphere can be corrected by determining an average pressure as a function of depth based on the draft of the vessel.

D. Electrode Materials

1. Anode Selection

The selection of anode materials for electrolysis of seawater is a considerable problem. If used as an anode, most metals tend to oxidize and go into solution as their metallic ions

$$M \rightarrow M^{2t} + 2e^{-}$$

There are very few materials which if made anodic will not participate in the reaction and corrode away. Furthermore, it is preferred that the electrode materials be chemcially inert in either the passive or active mode, i.e. have good corrosion resistance and halogen resistance qualities; be easily fabricated into thin bands or wires which will conform to the ship's hull; be inexpensive and commercially available; and be capable of withstanding high current densities and elevated voltages. For selection of an anode material, the choice is severely restricted. In commercial chlorinators, impressed current cathodic protection systems,[4] and electrochemical flotation oil separation systems[5] the materials used include graphite and noble metals or alloys such as platinum, platinized titanium, platinum-iridium alloys, platinized niobium,

and palladium.

Pure noble metal wire is prohibitively expensive and can be dismissed as an option for full-scale use (pure platinum wire, 5 mil diameter, at present market cost is approximately 55¢ a foot). Also pure platinum is quite soft. Even when allowed with iridium, it is difficult to work with.

Platinized wire is composed of a conducting core with a platinum coating. The platinized wire that is commercially available (Engelhard Industries) has a coating of platinum 50 micro-inches thick, and is considerably less expensive than pure platinum. It can withstand current densities of several thousand amperes per square foot. Platinized titanium is restricted to rather low driving voltages (up to 10 volts DC)[6] in the presence of chlorine ions because the titanium is attacked at any pores or bare areas when subjected to higher potentials. On the other hand, the niobium wire is stable in seawater up to 100 volts DC.[7] Another important factor to consider is that platinum is not totally inert, but tends to oxidize in the following reaction:

$$Pt + 6Cl^{-} \; [PtCl_6]^{-2}$$

Though the rate of oxidation will be very slow, it must be nonetheless be considered.

Graphite anodes are relatively inert in seawater and are quite inexpensive relative to anodes requiring noble metals. However, their use has three significant drawbacks. First, the resistivity of graphite is 1375.0 μΩ - cm (compared to 1.673 μΩ-cm for copper, 10.6 μΩ-cm for platinum, and 12.5 μΩ-cm for niobium). To achieve the same value of electrical resistance per unit length of electrode using graphite anodes the cross-section would have to be increased. This would necessitate using more material and having to mount larger electrodes on the hull. Because the surface area of the electrodes would be increased, the current density for a given total current would be decreased, resulting in larger bubble sizes. This is a further disadvantage because it is desired to maximize dispersion of the bubbles in the flow around the hull.

The second problem is that carbon also tends to oxidize in seawater, though it does so at a very slow rate. The oxidation reaction proceeds as follows:

$$C + O_2 \rightarrow CO_2$$

The theoretical chemical equivalent of graphite then is 4042 ampere-hours per pound, and the dissolution rate is 2.16 pounds per ampere per year. This is a low value compared to 20 lb/amp/yr for iron sacrificial anodes and 75 lb/amp/yr for lead. However, recalling that chlorine everpotential is lower than that of oxygen, chlorine evolution will predominate at lower current densities, and it is important to note that graphite is non-reactive in the presence of chlorine. Nonetheless, some dissolved oxygen will be present in the water near the electrode and will cause some dissolution of the anode. Brady(5), Baylor(3) and Kabanov(14) have all done work with graphite electrodes. They report that as the current density is increased, the increase in wettability caused by high polarization causes penetration into the pores of the electrode. The resulting chemical attack decreases the electrode's life. This effect can be reduced by filling the inner pores with an impregnant to limit the activity to the surface. Recommended impregnants include linseed oil, paraffin, opal wax (i.e. du Port de Nemours & Co.), or castor wax (Baker Castor Oil Company). A third problem with graphite is its brittleness and the

difficulty with which it is formed.

2. Cathode Selection

For choice of a cathode material the field is somewhat larger. The cathode should also be inert in seawater, have good corrosion resistance, and have the additional quality of being resistant to hydrogen embrittlement. The material which has been used successfully in electrochemical flotation oil separators is stainless steel, and this material is recommended for use in electrolytic drag reduction systems.

3. Prototype Electrode Installation

To best maximize the drag reduction the electrodes should be mounted as nearly flush with the hull as possible. The electrodes themselves would necessarily have to be thin wires or foil strips. The maximum admissible thickness of the electrode can be approximated by computing the admissible roughness for a rough, flat plate. The admissible roughness is that value below which the drag coefficient does not change and is computed as follows:

$$K_{adm} \leq \frac{100L}{R_{el}} \qquad (2.5)$$

$$K_{adm} \leq \frac{100\nu}{V_{max}}$$

ν = kinematic vicosity

V_{max} = maximum velocity

For a 300-foot destroyer escort with a maximum speed of 25 knots,

$$K_{adm} \leq (100) \frac{(1.05X10\text{-}5 \text{ ft}^2/\text{sec})(12 \text{ in/ft})}{(25 \text{ kt})(1.688 \text{ ft/sec})\text{-kt}}$$

$$K_{adm} \leq 0.299 \text{ mils}$$

Because this value is so very small, it may become necessary to inlay the electrodes and insulating backing to make it flush with the surface.

For reduced cost in installing the electrodes the anode and cathode could be affixed to an insulated backing "printed-circuit" fashion and these strips could then be mounted on the hull.

4. Electrodes used in Model-Testing Sequence

Because of the expense that would have been incurred using noble metal or other permanent anodes, most of the initial experiments were conducted using 5-mil diameter Nichrome wire. Nichrome does corrode when made anodic, however sufficient oxygen generation occurs for model-testing purposes. Experiments with graphite-coated tungsten wires were also conducted and they worked quite well for short periods of time. However, the graphite is oxidized too rapidly for

for the wire to be used in a series of model tests. In subsequent tests 1-mil platinum filaments were used as anodes. In all tests 5-mil copper wire or 2-mil copper foil was used as the cathodes.

III. POWER REQUIREMENT PREDICTION

The power requirement for generating a given current, (which determines the amount of gas produced at the electrodes and hence the amount of drag reduction) is dependent on several complex factors. Analysis of the factors permits optimization of the design parameters and development of techniques for prototype power requirement projections.

A. Theoretical Considerations

1. Decomposition voltage - A continuous current will flow between two electrodes only when the externally applied potential exceeds the "back potentials" of the electrodes. This voltage, termed the decomposition voltage, is the sum of several components, each of which is discussed below.

a. Oxidation and Reduction Potentials - A certain potential is required at the solid-electrolyte interface of each electrode for nucleation of the new phase. The oxidation and reduction potentials are the sum of the standard potentials, determined for an ideal solution of unit molality referenced to the hydrogen scale, and a correction to the standard potentials to account for the actual cell concentrations.

Standard oxidation potentials are tabulated in Reference (16). The correction is computed using the Nernst equation:

$$E_C = \frac{RT}{nF} \ln \frac{C_1}{C_2} \qquad (3.1)$$

R = Gas constant

T = Absolute temperature

F - Faraday's number

n = number of electrons participating in reaction

C_1, C_2 = Ionic concentrations of lower and higher oxidation states

Hence the oxidation potential can be computed as follows, (where the Nernst relation has been simplified and the temperature is assumed to be 25°C):

$$E = E_o - E_C$$

$$= E_o - \frac{0.0591}{n} \log \frac{[\text{Products}]}{[\text{Reactants}]} \qquad (3.2)$$

For the electrolysis of seawater the oxidation potentials are computed as follows (all computations assume the partial pressure of gas generated is 1 atmosphere - giving it a unit activity):

anode (oxidation half-reaction):

$2Cl^- \rightarrow Cl_2 + 2e^-$

$E_o = -1.3593$ volts

$$[Cl^-] = \left[\frac{18.980g}{100\ ml}\right]\left[\frac{1\ mole}{35.453g}\right] = 5.354 \times 10^{-4}N$$

$$E = E_o - \frac{0.0591}{n} \log \frac{(Pcl_2)}{[Cl^-]^2}$$

$$= -1.3595 + 0.0591 \log [Cl^-]$$

$$= -1.3595 - 0.1933$$

$E = -1.5528$ volts

Cathode (reduction half-reaction):

$$2H_2O + 2e^- \rightarrow H_2 + 2OH^-$$

$E_o = +0.828$ volts

pOH = 5.8

$$E = E_o + \frac{0.0591}{n} \log \frac{[OH^-]^2(P_{H2})}{[H_2O]}$$

$E = +0.485$ volts

The electrode potential for the cell is the algebraic sum of the oxidation potential of the anode and the reduction potential of the cathode or the difference of the two oxidation potentials. Hence the chlorine and hydrogen evolution of this potential is

$E = -1.553 + 0.485$ volts

$E = -1.068$ volts

This value assumes that only hydrogen is being generated at the cathode and only chlorine at the anode. These reactions will dominate, however as previously

mentioned, other reactions will occur at the electrodes if the potential is sufficient for the reaction to occur.

b. Polarization Voltage - Polarization is a shift in the voltage between electrodes due to the passage of current. It occurs because the gases formed at the electrodes are not set free entirely and a certain quantity is absorbed by the electrodes. This causes the electrodes to develop a back potential opposing the applied voltage. As the gases are accumulated the opposing potential increases. Kabanov states that in high velocity electrolytes (as would be the case where the electrodes are mounted on the hull of a moving ship) the effect of polarization is reduced because the reaction products do not accumulate and (although absorption by the electrodes will not be entirely eliminated) significant leaching of the electrodes will occur.[8]

c. Chemical Overpotential - Overpotential is the excess of the potential above the equilibrium value that must be applied to the electrochemical cell in order to maintain a finite current flow. This potential represents the excess of energy required to form the new phase. The magnitude of the overpotential is dependent on the electrode material (and whether

the electrode is an anode or cathode), the gases being evolved, and the current density. For small current densities, the overpotential can be approximately by a linear function of current density[9]. However, as the current density increases, the current density-overpotential relationship takes on the form:

$$E = a + b\ln J$$

Tafel developed the relationship:

$$E = 2.303 \frac{RT}{\alpha F} (\log J - \log J_o)$$

$$= \frac{0.0591}{\alpha} (\log J - \log J_o) \qquad (3.3)$$

Where α and J_o are empirically determined constants. Values of α and J_o for hydrogen and overpotentials for several products of electrolysis for numerous electrodes are tabulated in reference (9).

The values of α and J_o can be determined by plotting experimentally-obtained values of overvoltage for the particular product and electrode. Extrapolating the curve to the J axis yields the constant J_o. The slope of the curve is α.[10] Below J_o, the overvoltage is so low it can be assumed to be zero.

For chlorine generated at a platinized anode and hydrogen at a copper cathode, the constants are determined graphically in figure (1) below:

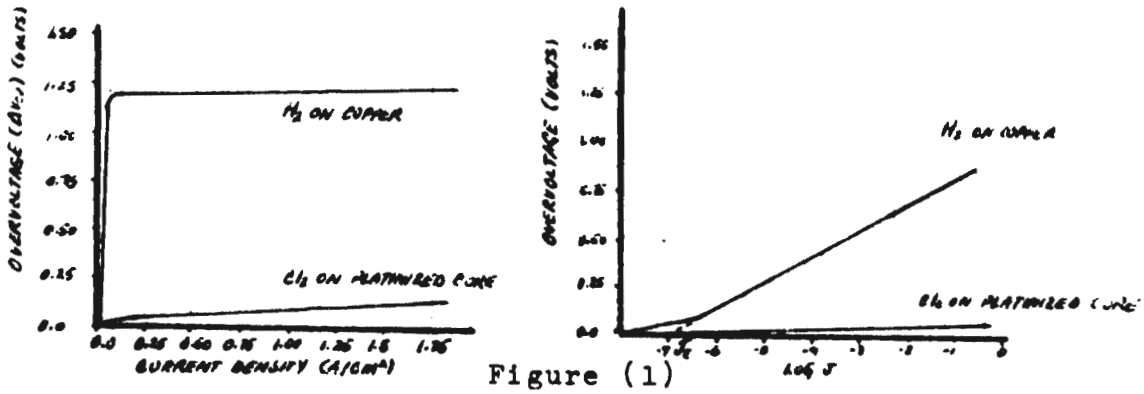

Figure (1)

For copper electrodes in alkaline electrolytes the overvoltage is slightly higher, however impurities in seawater lower this value.[11]

Several other factors affect the overvoltage, for a given elctrode material and electrolytic product. With the exception of the hydrogen overvoltage of platinized platinum, overvoltages decrease directly as the temperature increases.[12] For copper the change in hydrogen overvoltage with temperature for 0.4 amperes per square centimeter is tabulated below:

Hydrogen Overpotential (copper cathode) at 0.4 amperes/cm^2

Temperature (°C):	0.4	20.0	47.4	73.5
Overpotential (volts):	0.572	9.508	0.508	0.395

Measurements of the hydrogen overvoltage of copper for a range of pressures indicates that overvoltage decreases with pressure and is a hyperbolic relationship as shown in the following figure: :

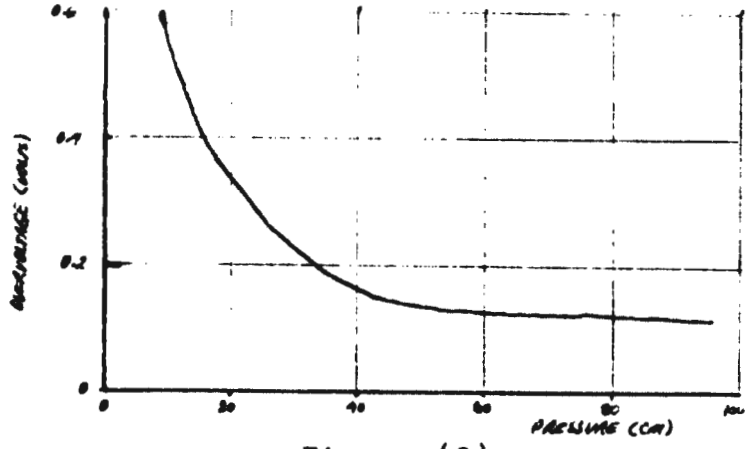

Figure (2)

Inspection of figure (2) shows that above a pressure of one atmosphere, the overpotential is asymptotic and decreases negligibly.

The hydrogen overvoltage of metals can be lowered by superimposing an alternating current on a direct current. This effect is apparently due to depolarization of the cathode by generation of the products of oxidation at the electrode. The extent

of the depolarization is determined primarily by the ratio of the alternating current to the direct current density. (9) Obviously, this technique could only be applied if both electrodes are platinum or some other material which will not ionize when made anodic.

d. Ohmic Potential Drop - As in any electrical circuit, there is an ohmic resistance associated with passage of current through material with a certain electrical conductivity. The potential drop occurs due to electrical energy being dissipated in the solution in the form of heat.

e. Summary - For analysis of the voltage-current relationship of the electrochemical circuit, the applied voltage can be expressed as follows:

$$V_{app} = E + \Delta V_{over\ v} + V_{ohmic}$$

V_{app} = applied voltage

E = oxidation-reduction potential

$\Delta V_{over\ v}$ = anode/cathode overpotentials

ΔV_{ohmic} = ohmic potential drop

Expanding this equation term by term yields

$$V_{app} = E(cathode) - E(anode) + \Delta V_{over\ v}(anode) + \Delta V_{over\ v}(cathode) + \Delta V_{ohmic}$$

where

$$E(\text{cathode}) = E_o - \frac{0.0591}{n} \log \frac{[\text{PRODUCTS}]}{[\text{REACTANTS}]}$$

$$E(\text{anode}) = E_o - \frac{0.0591}{n} \log \frac{[\text{PRODUCTS}]}{[\text{REACTANTS}]}$$

$$\Delta V_{\text{over v}}(\text{cathode} = \frac{0.0591}{\alpha_c} (\ln J - \ln J_{o,c})$$

$$\Delta V_{\text{over v}}(\text{anode}) = \frac{0.0591}{\alpha_a} (\ln J - \ln J_{o,a})$$

$$\Delta V_{\text{ohmic}} = IR_{\text{ohmic}}$$

B. Limiting Current

The voltage-current characteristic of a given electrochemical cell is affected by mass transfer processes which determine the amount of electroactive material supplied to the electrodes. Most of the literature in this field has been published by Russian workers, the most outstanding being Levich (reference 18). Other work has been done by Adams (1) and Riddiford (4). The following is summarized from these works.

In an electrochemical reaction the transfer of electrons in the oxidation and reduction reactions is actually composed of individual steps: the transfer of ions from the bulk of the solution to the electrode surface, the electrochemical reaction itself, the formation of the final product, and the removal of the final product from the electrode surface. The rate of electron transfer from anode to cathode is usually much faster than the rate of transfer from the reactants and hence it is the rate of mass transfer of the reactants to the electrodes which is usually the limiting step. Increasing the mass transfer rates increases the electron transfer rate, and if increased enough the electron transfer rate becomes limiting. Hence, the current in the circuit

for a given potential is velocity-dependent and has a limiting value, which is also velocity dependent. A typical current-voltage curve is diagrammed below.

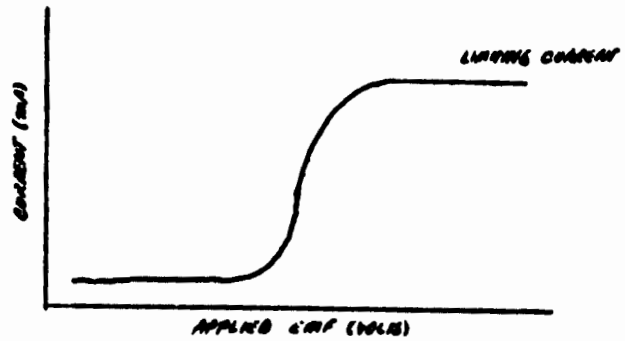

Mass transfer has three modes: migration, convection, and diffusion. Migration results from the force exerted on the charged particles by an electric field. In seawater where there is an excess of supporting electrolyte, this effect can be neglected. Convection occurs from motion of the flow past the electrodes and will be a predominant effect in determining the current expected from hull-mounted electrodes. Diffusion arises due to the concentration gradient existing between the bulk solution and the region near the electrode.

The general expression for the flux density of the ionic species A_j (neglecting migration) is given by

$$\vec{J} = C_j \vec{V} - D_j \text{ grad } C_j$$

D_j = diffusion coefficient of A_j

$\vec{V}$ = fluid velocity vector

C_j = concentration of A_j

Solving for $\frac{\partial C_j}{\partial t}$

$$\frac{\partial C_j}{\partial t} = \text{div } (D_j \text{ grad } C_j) - \vec{V} \text{ grad } C_j \quad (3.4)$$

Solution of equation (3.4) using appropriate boundary conditions permits the calculation of the maximum rate at which A_j can be transported. The difficulty arises in describing the velocity vector, $\vec{V}$, and the diffusion coefficient for the case of turbulent flow near a rough surface. Levich gives the approximate diffusional flux for this case as

$$J_D \approx \frac{(c_f)^{0.25} V^{0.5} D^{0.75} C_o}{\upsilon^{0.25} h^{0.5}}$$

c_f = coefficient of turbulent resistance

V = average velocity

D = effective coefficient of turbulent diffusion

C_o = bulk concentration

ν = kinematic viscosity

h = average protrusion dimension

The nature of several of the constants in this equation precludes its use except for first approximation analysis. But it is important to note that the diffusional flux is proportional to the square root of the velocity.

For a plate electrode in a flowing laminar solution Levich gives the equation:

$$i_{lim} = 0.68nFDC_0 b \left(\frac{\nu}{D}\right)^{0.33}\left(\frac{v_l}{\nu}\right)^{0.5} \quad (3.6)$$

where l is the length of the plate in the direction of the liquid flow and b is the width normal to the flow direction. This value of i_{lim} will be considerably lower than for the case of turbulent forced convection near a rough surface because less macroscopic mixing occurs, and the beneficial effects caused by protrusion of the electrode into the solution (if it is not flush with the hull) are neglected. However for purposes of obtaining a conservative design estimate equation (3.6) is satisfactory.

IV. MODELLING TECHNIQUES

A. Ohmic Resistance

For a single anode-cathode pair immersed in a conducting electrolyte, we can model the ohmic resistance of the electrochemical circuit as a ladder circuit of parallel and series resistors. The series resistors represent differential portions of the total electrode resistances and the parallel resistors represent differential resistances of the total electrolyte resistance. In determining the ohmic resistance, the oxidation-reduction potential and the overpotentials are neglected. (The following derivation was developed by Dr. Frederic I. Davis, Mathematics Dept., U. S. Naval Academy).

The circuit model is diagrammed below:

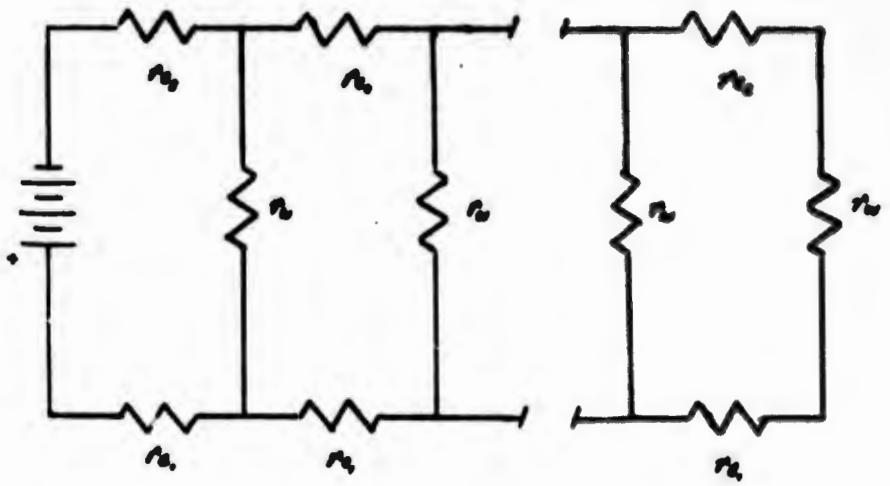

Figure (3)

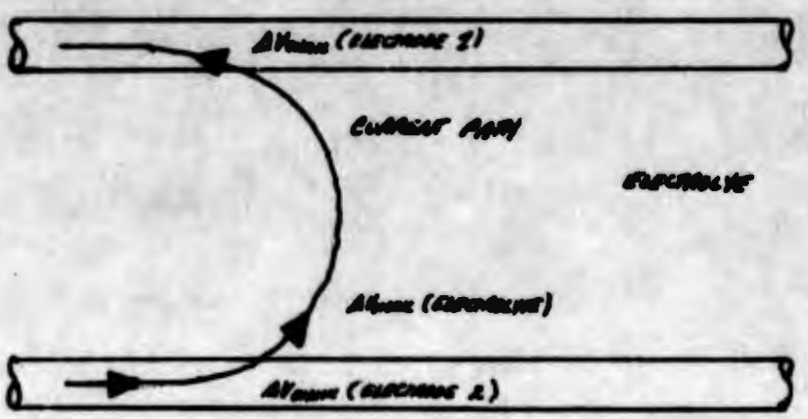

Figure (4)

The total electrolyte resistance between two cylindrical conductors of equal diameter is given by

$$R_W = \frac{\rho_W \cosh^{-1}(S/D)}{\pi L} \qquad (4.1)$$

ρ_W = electrolyte resistivity

S = electrode separation

D = electrode diameter

L = immersed electrode length

The derivation of this equation is found in Appendix (A).

The total resistance for each electrode can be computed using the equations:

$$R_{e_1} = \frac{\rho_{e_1} L}{A}$$

$$R_{e_2} = \frac{\rho_{e_2} L}{A}$$

ρ_{e_1}, ρ_{e_2} = electrode resistivity

L = electrode length

A = cross-sectional area

Defining an average R_e ,

$$R_e = \frac{(\rho_{e_1} + \rho_{e_2})}{2} \frac{L}{A}$$

Solving for the circuit model elements,

$$r_W = R_W n$$

and

$$r_e = \frac{R_e}{(n-1)}$$

where n is the number of "rungs" in the ladder network. It is desired to develop a recursion relation relation for expressing the resistance of (n+1) rungs of the network in terms of n rungs

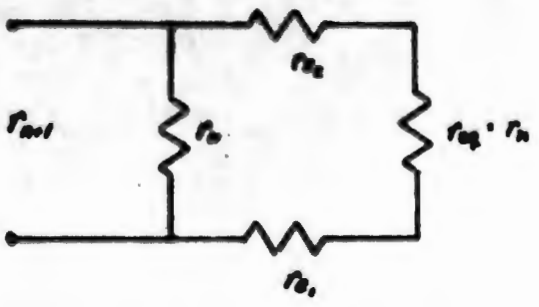

Figure (5)

Figure (6)

Considering the end parallel resistor,

$$r_1 = \frac{r_W}{1}$$

Expressing this relationship in matrix form

$$R_1 = \begin{vmatrix} r_W \\ 1 \end{vmatrix}$$

The expression for r_2 is

$$r_2 = \frac{r_W(r_1+2r_e)}{r_W+r_1+2r_e}$$

and it can be seen that for r_{n+1}

$$r_{n+1} = \frac{r_W(r_n+2r_e)}{r_W+r_n+2r_e}$$

In matrix form this relationship is

$$R_{n+1} = \begin{vmatrix} r_W & 2r_W r_e \\ 1 & r_W+2r_e \end{vmatrix} R_n$$

$$= MR_n$$

Since $R_n = M^{n-1}R_1$ it is desired to find a matrix T such that T diagnolizes M, i.e.

$$TMT^{-1} = \begin{vmatrix} \lambda_+ & 0 \\ 0 & \lambda_- \end{vmatrix}$$

and hence

$$M^p = T^{-1} \begin{vmatrix} \lambda_+^p & 0 \\ 0 & \lambda_-^p \end{vmatrix} T$$

Solving for the eigenvalues of M_{-1} and the values of $\lambda_{\pm}$

$$T^{-1} = \begin{vmatrix} 2r_w r_e & 2r_w r_e \\ r_e + \sqrt{r_e^2 + 2r_e r_w} & r_e - \sqrt{r_e^2 + 2r_e r_w} \end{vmatrix}$$

and

$$T = \frac{1}{\det} \begin{vmatrix} r_e - \sqrt{r_e^2 + 2r_e r_w} & -2r_w r_e \\ -r_e - \sqrt{r_e^2 + 2r_e r_w} & 2r_w r_e \end{vmatrix}$$

Substituting

$$M^p = \frac{1}{\det} \begin{vmatrix} 2r_e r_w & 2r_e r_w \\ r_e + \sqrt{} & r_e - \sqrt{} \end{vmatrix} \cdot \begin{vmatrix} (r_w + r_e + \sqrt{})^p & 0 \\ 0 & (r_w + r_e - \sqrt{})^p \end{vmatrix}$$

$$\cdot \begin{vmatrix} r_e - \sqrt{} & -2r_w r_e \\ -r_e - \sqrt{} & 2r_w r_e \end{vmatrix}$$

where $\sqrt{} = \sqrt{r_e^2 + 2r_e r_w}$

Expanding and substituting for r_n

$$r_n = r_w \frac{(r_e + \sqrt{})(r_w + r_e + \sqrt{})^{n-1} - (r_e - \sqrt{})(r_e + r_w - \sqrt{})^{n-1}}{(r_w + r_e + \sqrt{})^n - (r_w + r_e - \sqrt{})^n}$$

Recalling that $r_e = \frac{R_e}{(n-1)}$ and $r_w = R_w n$, substituting, and taking the limit as n approaches infinity

$$R_n = \frac{\sqrt{2R_w R_e} + \sqrt{2R_w R_e}\exp\left(\sqrt{\frac{8R_e}{R_w}}\right)}{1 - \exp\left(\sqrt{\frac{8R_e}{R_w}}\right)}$$

The expression for the ohmic resistance of the circuit is

$$R = \sqrt{2R_e R_w}\coth\sqrt{\frac{2R_e}{R_w}} \qquad (4.2)$$

B. Total Circuit Resistance

A closed-form solution can be developed for "first approximation" analysis of voltage and current relationships for cylindrical electrodes. The circuit is modelled in a manner similar to the method developed for determing ohmic resistance however the oxidation-reduction potential is modelled as a back DC voltage source and the overvoltage for the limited range of current densities involved is assumed to be a current-dependent voltage source, where the dependence is assumed to be linear. Inspection of Figure (4) indicates that this assumption is justified.

The circuit model is diagrammed below

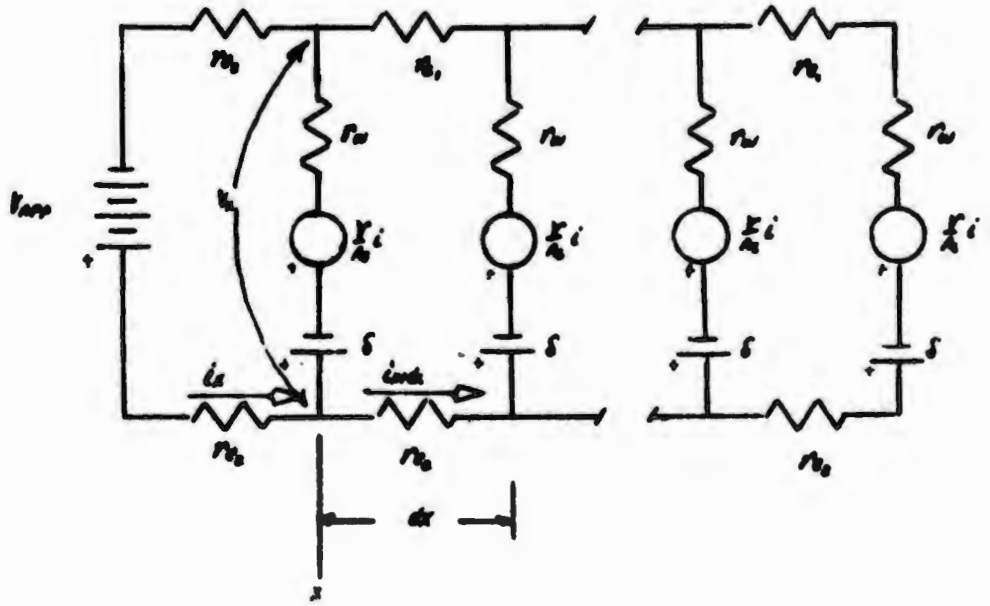

Figure (7)

The expression for the total electrolyte resistance is given by

$$R_w = \frac{a}{L}$$

A differential resistance would be

$$r_w = \frac{a}{dx}$$

The expressions for the total resistance of each electrode are

$$R_{e_1} = \beta_1 L$$

$$R_{e_2} = \beta_2 L$$

Similarly

$$r_{e_1} = \beta_1 dx$$

$$r_{e_2} = \beta_2 dx$$

Defining an average r_e and β

$$r_e = \frac{\beta_1 + \beta_2}{2} dx = \beta dx$$

The expression for the sum of the oxidation-reduction potential and the overpotential is assumed to have the form

$$\Sigma\Delta V = \frac{\gamma}{A} i_x + \delta$$

where the constants γ and δ are graphically determined as follows:

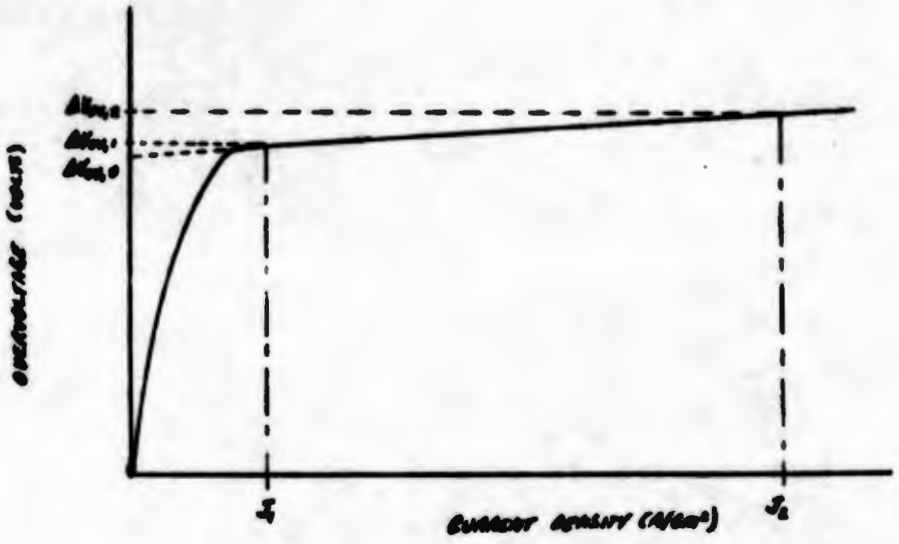

Figure (8)

Hence,

$$\frac{\gamma}{A_s} i_x + \delta = E + \frac{(\Delta V_{ov,2} - \Delta V_{ov,1})}{(J_2 - J_1)} j + \Delta V_{ov,0} \quad (4.3)$$

E = oxidation-reduction potential

A_s = electrode surface area

j = current density

ΔV_{ov} = values from graph, composite overvoltage

where

$$\gamma = \frac{\Delta V_{ov,2} - \Delta V_{ov,1}}{J_2 - J_1} \quad (4.4)$$

$$\delta = E + \Delta V_{ov,0} \quad (4.5)$$

Returning to the circuit model, Kirchoff's current equation at x is

$$i_{x+dx} = i_x - \frac{[V_x - (\frac{\gamma}{A_s} i_x + \delta)]}{\alpha} dx \qquad (4.6)$$

Applying Fourier's expansion to the i_{x+dx} term, and neglecting all but the first-order term

$$i_{x+dx} = i_x + \frac{di_x}{dx} (dx)$$

substituting into equation (4.6) and solving for V_x

$$V_x = -\alpha \frac{di}{dx} + \frac{\gamma}{A_s} i_x + \delta \qquad (4.7)$$

Kirchoff's voltage equation at x is

$$V_{x+dx} = V_x - 2i_x \beta dx$$

Applying Fourier's expansion, substituting, and solving for i_x

$$i_x = -\frac{1}{2\beta} \frac{dV_x}{dx} \qquad (4.8)$$

Combining equations (4.7) and (4.8) gives

$$\frac{d^2V}{dx^2} - \frac{\gamma}{\alpha A_s} \frac{dV}{dx} - \frac{2\beta}{\alpha} V = -\frac{2\beta\delta}{\alpha} \qquad (4.9)$$

The general solution of this linear differential equation has the form

$$V(x) = Ae^{\lambda_1 x} + Be^{\lambda_2 x} + \delta \qquad (4.10)$$

where

$$\lambda_1 = \frac{\gamma}{2\alpha A_s} - \frac{1}{2\alpha}\left(\frac{\gamma^2}{A_s^2} + 8\beta\alpha\right)^{1/2}$$

$$\lambda_2 = \frac{\gamma}{2\alpha A_s} + \frac{1}{2\alpha}\left(\frac{\gamma^2}{A_s^2} + 8\beta\alpha\right)^{1/2}$$

The current equation, derived from equation (4.8) is

$$i(x) = -\frac{A\lambda_1}{2\beta} e^{\lambda_1 x} - \frac{\beta\lambda_2}{2\beta} e^{\lambda_2 x} \qquad (4.11)$$

The first boundary condition is that a finite current flows through the last parallel resistor at $x = L$. The second boundary condition is that the voltage at $x = L$ exceeds the decomposition voltage. Taken together these two conditions imply that gas bubble evolution occurs at all points on the length of the conductors.

Applying the boundary conditions

$$\text{at } x = L, \quad i(x) = I_i$$

$$\text{at } x = L, \quad v(x) = \frac{\gamma}{A_s} I_i + \delta$$

the constants A and B are

$$A = \frac{-\left(\frac{\gamma}{A_s}\lambda_2 + 2\beta\right)}{(\lambda_1 - \lambda_2)} I_i e^{-\lambda_1 L}$$

$$B = \frac{\left(\frac{\gamma}{A_s}\lambda_1 + 2\beta\right)}{(\lambda_1 - \lambda_2)} I_i e^{-\lambda_2 L}$$

Substituting into equations (4.10) and (4.11) the voltage and current equations are

$$V(x) = \frac{\left(\frac{\gamma}{A_s}\lambda_2+2\beta\right)}{(\lambda_2-\lambda_1)} I_i e^{\lambda_1(x-L)} - \frac{\left(\frac{\gamma}{A_s}\lambda_1+2\beta\right)}{(\lambda_2-\lambda_1)} I_i e^{\lambda_2(x-L)} + \delta \qquad (4.12)$$

$$i(x) = \frac{-\left(\frac{\gamma}{A_s}\lambda_2+2\beta\right)}{(\lambda_2-\lambda_1)} \frac{I_i\lambda_1}{2\beta} e^{\lambda_1(x-L)} + \frac{\left(\frac{\gamma}{A_s}\lambda_1+2\beta\right)}{(\lambda_2-\lambda_1)} \frac{I_i\lambda_2}{2\beta} e^{\lambda_2(x-L)} \qquad (4.13)$$

The applied voltage and total current are computed for $x = 0$ and are

$$V_o = \frac{\left(\frac{\gamma}{A_s}\lambda_2+2\beta\right)}{(\lambda_2-\lambda_1)} I_i e^{\lambda_1 L} - \frac{\left(\frac{\gamma}{A_s}\lambda_1+2\beta\right)}{(\lambda_2-\lambda_1)} I_i e^{\lambda_2 L} + \delta \qquad (4.14)$$

$$I_o = \frac{-\left(\frac{\gamma}{A_s}\lambda_2+2\beta\right)}{(\lambda_2-\lambda_1)} \frac{I_i\lambda_1}{2\beta} e^{\lambda_1 L} + \frac{\left(\frac{\gamma}{A_s}\lambda_1+2\beta\right)}{(\lambda_2-\lambda_1)} \frac{I_i\lambda_2}{2\beta} e^{\lambda_2 L} \qquad (4.15)$$

The total circuit resistance is the ratio of V_o to I_o.

Expressing equations (4.12) and (4.13) in terms of the non-dimensional parameters

$$\eta = \frac{\gamma^2}{R_w R_e A_s^2}$$

$$\kappa = \frac{R_e A_s}{\gamma}$$

$$\xi = \frac{x}{L}$$

and defining J_L as the current density corresponding to I_L/A_s (where the minimum value of J_L is J_1, determined from figure ( ))

$$V(\xi) = \frac{\gamma J_L}{2}\left[\frac{(\eta+4)}{\eta^{1/2}(\eta+8)^{1/2}} + 1\right] \cdot \exp\left\{\frac{\kappa\eta^{1/2}}{2}\left[\eta^{1/2}-(\eta+8)^{1/2}\right](\xi-1)\right\} - \frac{\gamma J_L}{2}\left[\frac{(\eta+4)}{\eta^{1/2}(\eta+8)^{1/2}} - 1\right] \cdot \exp\left\{\frac{\kappa\eta^{1/2}}{2}\left[\eta^{1/2}+(\eta+8)^{1/2}\right](\xi-1)\right\} + \delta \quad (4.16)$$

$$i(\xi) = -\frac{J_L A_s \eta^{1/2}}{8}\left[\eta^{1/2}-(\eta+8)^{1/2}\right]\left[\frac{(\eta+4)}{\eta^{1/2}(\eta+8)^{1/2}} + 1\right] \cdot \exp\left\{\frac{\kappa\eta^{1/2}}{2}\left[\eta^{1/2}-(\eta+8)^{1/2}\right](\xi-1)\right\} + \frac{J_L A_s \eta^{1/2}}{8}\left[\eta^{1/2}+(\eta+8)^{1/2}\right]\left[\frac{(\eta+4)}{\eta^{1/2}(\eta+8)^{1/2}} - 1\right] \cdot \exp\left\{\frac{\kappa\eta^{1/2}}{2}\left[\eta^{1/2}+(\eta+8)^{1/2}\right](\xi-1)\right\} \quad (4.17)$$

In using these equations for predictions, values of current density (i/A_s) for various positions along the conductor should be computed to verify that the range of current densities does in fact fall within the range for which the overvoltage is assumed linear. An iterative procedure may be necessary to refine the overpotential parameters and I_L to make the results fit the original assumptions.

Of considerable significance is the change in current density with position along the electrode length. The change in current density represents the current passing to the electrolyte from the electrode and hence is proportional to the volume of gas being generated per unit length of electrode. Preferably the current density over the entire length of the electrodes should be uniform, in order to insure uniform gas bubble production at all places on the hull.

The change in current density with distance along the conductors is computed from equation (4.7):

$$\frac{di}{dx} = \frac{\frac{\gamma}{A} i - V + \delta}{a}$$

This equation reduces to

$$\frac{di}{dx} = -\frac{(\frac{\gamma}{A_s}\lambda_2+2\beta)(\frac{\gamma}{A_s}\lambda_1+2\beta)I_L}{2a\beta(\lambda_2-\lambda_1)}[e^{\lambda_1(x-L)} - e^{\lambda_2(x-L)}] \quad (4.18)$$

Non-dimensionalizing, and introducing the non-dimensional variable $\nu = \frac{R_w A_s}{\gamma}$

$$\frac{di}{d\xi} = \frac{-J_L A_s \eta^{1/2}}{8\nu L}[\eta^{1/2} - (\eta+8)^{1/2} + 4\eta^{-1/2}][\frac{(\eta+4)}{\eta^{1/2}(\eta+8)^{1/2}} + 1] \cdot$$

$$\exp\{\frac{\kappa\eta^{1/2}}{2}[\eta^{1/2} - (\eta+8)^{1/2}](\xi-1) \qquad (4.19)$$

$$+ \frac{J_L A_s \eta^{1/2}}{8\nu L}[\eta^{1/2} + (\eta+8)^{1/2} + 4\eta^{-1/2}] \cdot$$

$$[\frac{(\eta+4)}{\eta^{1/2}(\eta+8)^{1/2}} - 1] \cdot$$

$$\exp\{\frac{\kappa\eta^{1/2}}{2}[\eta^{1/2} + (\eta+8)^{1/2}](\xi-1)\} \qquad (4.20)$$

The absolute value of $\frac{di}{dx}$ is proportional to the distribution of bubbles being generated on the conductors. It is significant to note that the change in distribution is inversely proportional to the length of the conductors and to the ratio $\nu = \frac{R_w A_s}{\gamma}$. This latter condition is intuitive, for as the value of R_w decreases, obviously the current will tend to "leak out" of the anode at a greater rate.

Due to the complex nature of the overpotentials involved in electrolysis, computer modelling of the electrochemical circuit is the only technique for achieving truly accurate results.

A computer program (ILOOP, in Basic, appendix B) models the circuit in a manner similar to the model used for developing the closed form solution, however it models the overvoltage as a current-dependent DC voltage source where the relationship is assumed logarithmic. The circuit is diagrammed below:

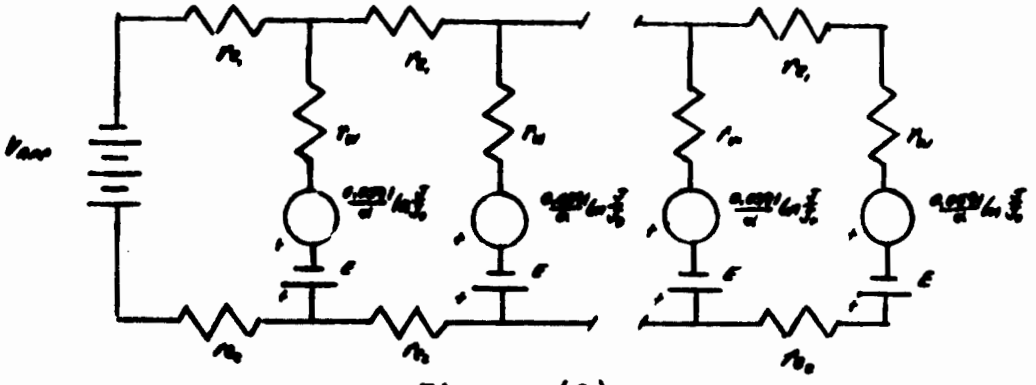

Figure (9)

Input data for running the program include values of anode, cathode, and electrolyte resistivity; the oxidation-reduction potentials; the values of the empirical constants α and J_o for the anodic and cathodic reactions (equation (3.3)); electrode length and separation, and a desired number of Δx divisions, corresponding to incremental lengths of the conductors.

The program first computes the values of the circuit resistors, r_e and r_s by dividing the respective total resistance values by the number of Δx divisions. It then determines the value of the

back DC voltage due to the oxidation and reduction potentials.

The program next determines the minimum applied voltage necessary to insure that the potential difference at every point on the the electrodes exceeds the decomposition voltage. Initially, a small current (corresponding to the smallest value of the two values of J_o in the overpotential equations) is assumed to flow through the end parallel resistor of the circuit. By successive iterations the minimum applied voltage is computed as well as the corresponding decomposition resistance and minimum current.

Following these initial steps, values of total voltage and current for an input range of values of I_L (previously estimated using the closed-form solution) can be computed.

V. DESIGN OPTIMIZATION

In order to optimize the configuration of the electrodes a myriad of inter-related trade-offs must be analyzed. The two principal objectives to be considered in developing a design are even distribution of the gas bubbles generated at the electrodes over the surface of the hull and maximization of the current produced for a given applied voltage. Each of these topics will be considered separately.

A. Power Requirements

The factors which affect the current produced in the electrolytic cell include the resistivity of the electrodes and electrolyte; the dimensions and separation distance of the electrodes; the values of the oxidation-reduction potential and overpotential for the particular reaction and electrode materials; and the applied voltage. Inspection of equations (4.16) and (4.17) indicates that increasing the value of the non-dimensional parameter η (which, in physical terms, is the ratio of the "chemical" resistance due to the overpotential to the constituent ohmic resistances) will result in a decrease in the circuit resistance. The variation of circuit resistance for a sample set of variables is presented in figure (10). The variation

of η with several design parameters is diagrammed below:

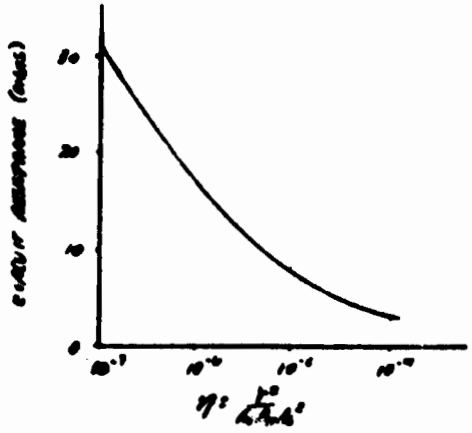

Figure (10)

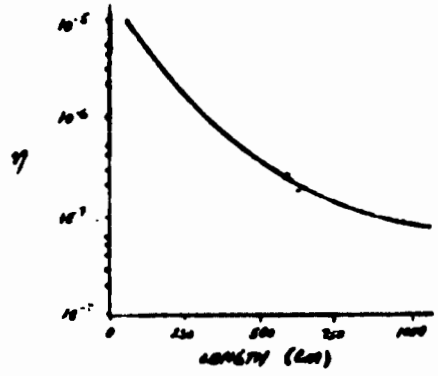

Figure (11)

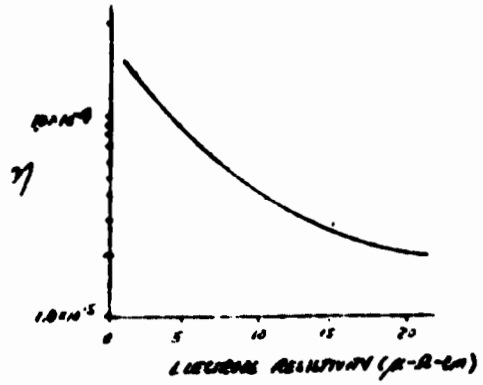

Figure (12)

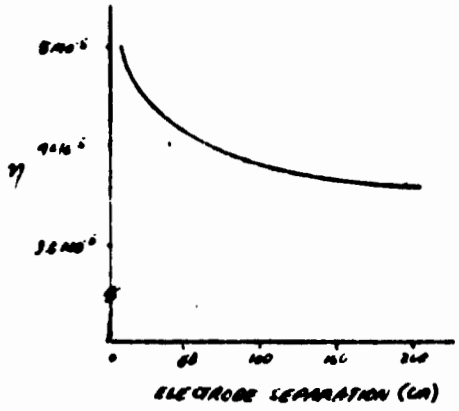

Figure (13)

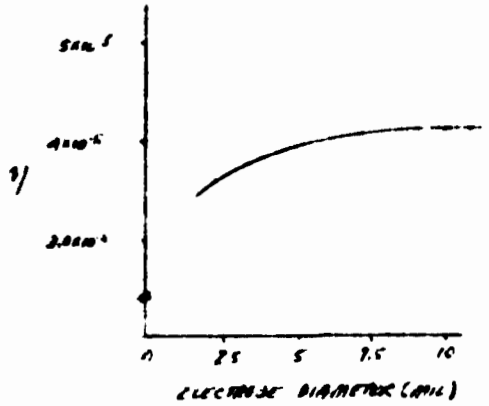

Figure (14)

It can be seen that the current will be increased for a given voltage if the resistivity of the electrodes and electrolyte, the length of the electrodes, and if the electrode separation distance can be reduced; and if the diameter of the electrodes is increased.

A significant reduction in the total circuit resistance is achieved by connecting the electrode pairs in parallel. As the number of pairs connected in parallel is increased the voltage required to produce a given current approaches the decomposition voltage, which is the theoretical limit. This assumption of course infers that the potential drop due to connecting wires is negligible and that the electrode is configured such that the potential difference between any two points on the electrode pair is uniform. This latter topic will be discussed in more detail in the next section.

In determining the design current for a given electrode pair several factors must be taken into account. First, if the limiting current is not to be exceeded, then this condition must be met. Second, if the current density at the end of the electrode pair is not to be less than a specified minimum, then this must

be considered. Third, the velocity dependence of the current must be taken into account.

B. Bubble Distribution

The separation distance and length of the electrodes as well as their placement on the hull will affect the resulting distribution of bubbles in the flow around the hull. Increasing the value of η causes a more dramatic drop-off rate with length to occur. The decrease in current density with electrode length can be offset by several methods. The electrode length can be decreased, however this will neccessitate using insulated connecting wires to insure that electrodes transverse the full girth of the hull. A second technique is to design for a voltage which is in excess of the voltage corresponding to the limiting current. In this design the current will remain constant regardless of the applied voltage for a portion of the electrode's length. The drawback to this technique is that it results in a considerable waste of power. The remaining proposed technique is to vary the cross-sectional area of the electrodes with distance away from the point where the electrodes are connected to the voltage source. If ribbon electrodes

are used, where the width of the strip is an increasing function of length, then the resistance of the conductor will decrease as the inverse of its length. When the resistance of the conductor is comparable to that of the electrolyte, (as is the case with seawater) the effect on the change in the current density will be significant. It will also reduce the dependence of potential difference betwen the electrodes with distance, which decreasesthe power requirements for the designed current. Difficulties arise in modelling this physical situation because the resistance of the electrolyte is dependent on the lateral dimensions of the electrodes and the differential equation describing the model becomes transcendental. Analysis of the voltage-current relationships for ribbon electrodes is incomplete as of this writing and will be the subject of a subsequent paper.

The location of the electrodes on the hull is determined by the characteristics of the flow around the particular hull. Visual and photographic analysis of the bubble distribution resulting in the flow around the 5-foot model.for various configurations and for a range of speeds indicated that the optimum configuration is one in which a large portion of the electrode pairs

are mounted forward on the hull and just aft of points of flow separation. In this manner a maximum number of bubbles are injected initially into the flow and bubbles lost by separation at various points on the hull are replaced. Furthermore, the electrodes are mounted normal to the direction of the flow in order to make the distribution more uniform with respect to girth. (A principal objection to mounting the electrodes parallel to the flow is that it is desired to reduce the effects of concentration overpotential arising from an accumulation of gas products at points farther aft on the electrodes.)

One other consideration is theorized but has not been analyzed completely to date. The injection of bubbles into the flow not only reduces the viscous resistance but may also reduce the wave-making drag by damping the amplitude of the waves generated by motion of the vessel. If such is the case, the electrodes should be mounted based on alaysis of the wave profile characteristic of the vessel.

VI. MODEL TESTS

A. Model Configuration

The configuration which was tested on the 18'2" model is depicted in the photographs in Appendix (D). The major bank of electrodes was located foward on the hull with two other banks located at the shoulders. The

remaining electrodeswere mounted in sets of two spaced evenly over the length of the hull.

The model was tested in fresh water, hence the drop-off effect of the current density is not significant enough to merit using shortened electrodes or varying-width ribbon electrodes. However, to irsure more uniformity in the bubble distribution, only alternate electrode pairs were connected to the voltage source on the same side of the hull. Hence for each set of two pairs, the bubble distribution is essentially uniform.

The 18'2" model was originally intended to have a total of sixty anode-cathode pairs. However time limitations and difficulties encountered in working with the platinum filament resulted in only thirty-three electrolytic cells actually being effective.

B. Experiment

In the final test, the model was towed in the Naval Ship Research and Develop Center's David Taylor Model Basin. The towing speeds ranged from 0.85 ft/sec and the current was varied between 0 and 4 amperes for each towing speed. The flow adjacent to the hull was turbulent over most of the hull length, even at lower speeds, because the leading electrode acted as a boundary layer trip.

The experiment was designed to test the effectiveness of the model configuration and to measure the effect of velocity on the power requirements. The former is considered first. The data are presented in figure (15) where the total drag is shown as a function of towing speed. By increasing the speed for the fixed value of current the percent drag reduction varied from 3.2% at the lower towing speeds to 17.5% in the middle of the speed range. With increasing speed the bubble injection had a diminishing effect, causing 2.3% drag reduction at the higher speed.

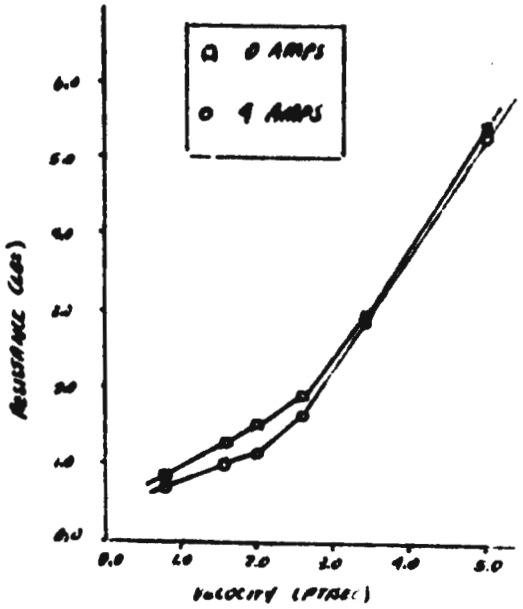

Figure (15)

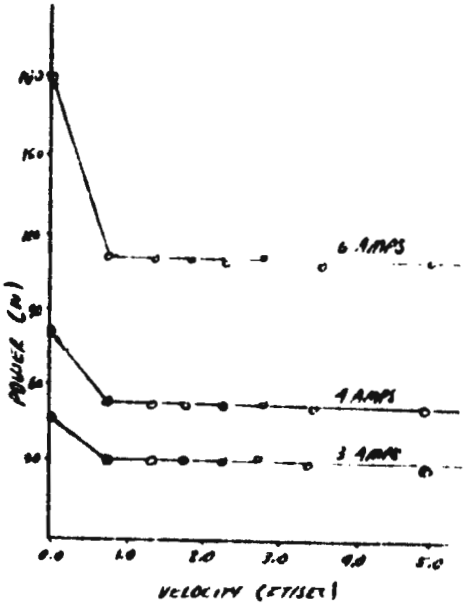

Figure (16)

The data for the power requirements necessary to maintain a constant current of four amperes for the range of towing speeds is presented in figure (16). The voltage required initially decreases dramatically with speed. It continues to decrease with speed, but at a reduced rate. At the speed at which maximum drag reduction occurred, the power required was 50.4 watts.

To demonstrate the velocity dependence on the input power required, the drag data is presented in figure (17) as the percent change in the ratio of EHP to input power as a function of velocity, and in figure (18) as the percent change in the coefficient of total resistance as a function of the ratio of velocity to input power.

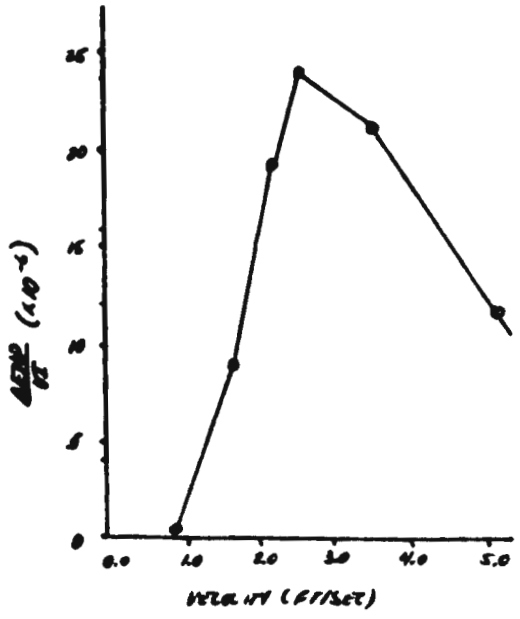

Figure (17)

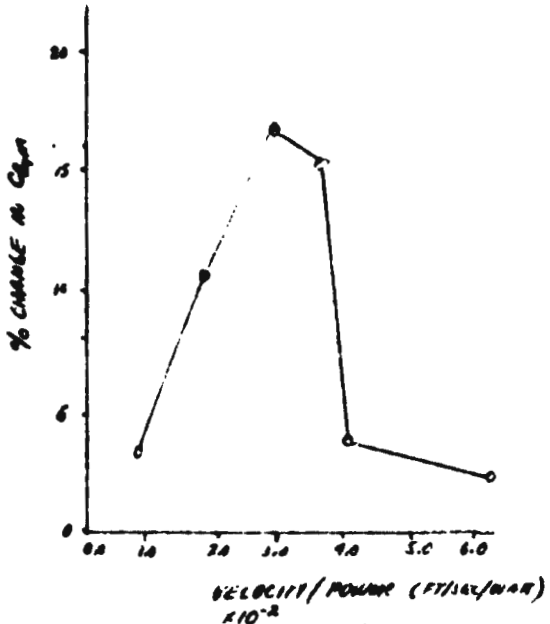

Figure (18)

VII. CONCLUSIONS

The results of the experiment verify the conclusions reached by McCormick and Bhattacharrya in their initial experiments. The magnitude of the drag reduction is a function of towing speed, the rate of gas bubble production and the configuration of the electrodes with respect to the flow around the hull. However, since no laminar flow conditions existed in the testing sequence for the 18'2" model, the lubricating effects of the gas bubbles in laminar flow were not observed. As the flow velocity increases the momentum absorption effect increases with velocity. After reaching a peak, the effects of momentum absorption decrease with increasing velocity and approach a limit.

However, one factor not considered in previous papers is the beneficial effect in reducing the input power that is derived from increased mass transport of electroactive material to the electrodes due to increased velocity. Hence the non-dimensional ratio of mass flow rate of the wake to mass flow rate of gas is not a valid parameter since it does not indicate the dependence of circuit resistance on the mass flow of the wake.

VIII PROTOTYPE PROJECTIONS

Due to the complexities inherent in predicting the power requirements and the lack of data on overvoltages in seawater, only testing of an actual prototype will provide accurate data. Furthermore, a maximum of 4 amperes was used in the model tests, hence the maximum possible drag reduction for the range of speeds tested was not determined. For the same reason the drag reduction effect at higher towing speeds was not determined.

Comparison of the data obtained by Bhattacharyya and McCormick on a model destroyer hull with the data obtained in the 18'2" model tests indicates that the effect of the bubbles on drag reduction is related to the wetted surface area of the model. Hence to achieve the same percentage drag reduction on a full-size hull at the same speed the current required would be approximately 65 amperes. Theoretically (assuming the electrodes can ebdesigned so that the potential difference between them is everywhere approximately equal, and assuming that there are a large number of cells connected in parallel) the voltage required to generate the necessary current would be equal to the oxidation-reduction potential and the overvoltage. Since the oxidation reduction for hydrogen and chlorine production 1.068 volts, and for a

maximum current density of 3 amperes/cm^2 for each electrode the overvoltage on platinized electrodes is approximately 3 volts. Hence the total voltage required would be 4 volts. An additional 2 volts should be added to take into account the effect of resistances external to the the electrolytic cells. Without considering the effect of the decrease in circuit resistance that occurs due to the vessel's motion, the power requirement is estimated to be 0.39 KW (which corresponds to 0.52 horsepower).

It is readily apparent that the results of this experiment indicate that drag reduction by electrolysis can effect a drag reduction that is dramatic relative to the power required to make it function. Vessels equipped with electrodes for drag reduction will realize sighificant savings in fuel and will have increased cruising ranges as a result of this fuel economy. Furthermore, as previously mentioned, the need for anti-fouling coatings will be reduced because the reaction products are toxic to fouling organisms. It can be expected then, that the vessel will not experience the increase in resistance that normally occurs with time out of drydock.

IX. FURTHER STUDY

The following topics are proposed for further study:

(1) Scale Effects - Due to the fact that the U.S. Naval Academy towing tank is only 125' long it is difficult to monitor the current over a range of model speeds. Hence further tests on the 18'2" model should be conducted in seawater over a wider range of speeds and for several different values of current.

(2) Ribbon Electrodes - Tests should be conducted to determine the optimum dimensions and spacing for variable width ribbon electrodes to insure uniform minimum potential difference over the length of the conductors and uniform bubble production in seawater.

(3) Conductivity in Flowing seawater - Tests should be conducted to determine the change in circuit resistance in flowing seawater at various speeds.

(4) Target Strength - SONAR Self Noise - The effect of electrolytic drag reduction on the sonar capabilities of Navy ships and target strengths of echo returns from ships equipped with the drag-reducing system should be investigated.

(5) Long-Run Cost Effectiveness - An analysis of the long-run savings in fuel and machinery weight versus initial

expenditures should be undertaken to determine the economy resulting in installation of the drag-reducing system.

FOOTNOTES

1 Yo. A. Buevich, "Drag Reduction Model for Particle Injection into a Turbulent Viscous Fluid Stream," Fluid Dynamics, 5, (March-April 1970), p. 271.

2 Ibid., p. 271.

3 M. McCormick, R. Bhattacharyya, and L. Sawyer, "Drag Reduction of a Deep Submergence Vehicle by Electrolysis," International Conference on Engineering in the Ocean Environment, IEEE, September 1973.

4 Gene D. Brady, "Graphite Anodes for Impressed Current Cathodic Protection: A Practical Approach," Materials Protection and Performance, 10 (October 1971), p. 20.

5 Q. H. McKenna, H. Helbar, L. M. Carrell, and R. F. Tobias, "Electrochemical Flotation Concept for Removing Oil from Water," Technical Report for Project 4305, Contract No. DOT-CG-24288-A, U.S. Coast Guard Office of Research and Development,1973, pp. 6-7.

6 Ibid., p. 7.

7 Ibid., p. 7.

8 Boris N. Kabanov, Electrochemistry of Metals and Adsorption, (Holon, Israel: Freund Publishing House, 1969), p. 41.

9 Veniamin G. Levich, Physiochemical Hydrodynamics, Trans., Scripta Technica, Inc., (Englewood Cliffs, N. J.: Prentice-Hall, Inc., 1962), p. 251.

[10] H. Jermanin Creighton, Principles of Electrochemistry, (New York: John Wiley and Sons, Inc., 1943), I, p. 252.

[11] Ibid., p. 245.

[12] Ibid., p. 253.

REFERENCES

1. Adams, Ralph N., Electrochemistry at Solid Electrodes, New York: Marcel Dekker, Inc., 1969.

2. Bhattacharya, Amit, and John H. Lienhand, "The Similarity of Bubble Growth in Boiling and Electrolysis" Technical Report AD707432, University of Kentucky, 1970.

3. Bokris, John O'M. and B. E. Conway, Modern Aspects of Electrochemistry, Vol. 6, New York: Plenum Press, 1971.

4. Bockris, John O'M. and Amulya K. N. Reddy, Modern Electrochemistry, 2 Vols., New York: Plenum Press, 1970.

5. Brady, Gene D., "Graphite Anodes for Impressed Current Cathodic Protection: A Practical Approach," Materials Protection and Performance, 10, No. 10 (October 1971), p. 20.

6. Buevich, Yo.A., "Drag Reduction Model for Particle Injection into a Turbulent Viscous Fluid Stream," Fluid Dynamics, 5, No. 2 (March-April 1970), pp. 271-276.

7. Comstock, John P., ed., Principles of Naval Architecture, New York: The Society of Naval Architects and Marine Engineers, 1967.

8. Corson, Dale R. and Paul Lorrain, Introduction to Electromagnetic Fields and Waves, San Francisco: W. H. Freeman and Co., 1962.

9. Creighton, H. Jermanin, Principles and Application of Electrochemistry, 2 Vols., New York: John Wiley and Sons, Inc., 1943.

10. Delahay, Paul, ed., Advances in Electrochemistry and Electrochemical Engineering, Vol. 4, New York: John Wiley and Sons, Inc., 1966.

11. Dwight, Herbert B., Electrical Coils and Conductors New York: McGraw Hill Book Co., Inc., 1945.

12. Glasstone, Samuel and David Lewis, Elements of Physical Chemistry, Princeton, N.J.: D. Van Nostrand Co., Inc., 1960.

13. Harrington, A.R., Introduction to Electromagnetic Engineering, New York: McGraw-Hill Book Co., 1958.

14. Kabanov, Boris N., Electrochemistry of Metals and Absorption, Holon, Israel, Freund Publishing House, 1969.

15. Lap, A.W.J. "Biliography on Ship Resistance," International Towing Tank Conference, Berlin/ Hamburg, Germany, 1972.

16. Latimer, Wendell M., Oxidation Potentials, Englewood Cliffs, N.J.: Prentice-Hall, Inc. 1952.

17. Lingame, James J., Electroanalytical Chemistry, New York: John Wiley & Sons, Inc., 1958.

18. Levich, Veniamin G., Physiochemical Hydrodynamics, Trans., Scripta Technica, Inc., Englewood Cliffs, N.J.: Prentice-Hall, Inc., 1962.

19. Lumley, J.L., "The Reduction of Shin Friction Drag," Fifth Office of Naval Research Symposium on Naval Hydrodynamics, Bergen, Norway, 1964, pp. 915-946.

20. McCormick, M. and R. Bhattacharyya, "Drag Reduction of a Submersible Hull by Electrolysis," Naval Engineers Journal, (April 1973), pp. 11-16.

21. McCormick, M., R. Bhattacharyya, and L. Sawyer, "Drag Reduction of a Deep Submergence Vehicle by Electrolysis" International Conference on Engineering in the Ocean Environment, IEEE, September 1973.

22. McKenna, Q.H., H. Helber, L.M. Carrell, and R.F. Tobias, "Electrochemical Flotation Concept for Removing Oil from Water," Technical Report for Project 4305, Contract No. DOT-CG-24288-A, U.S. Coast Guard Office of Research and Development, 1973.

23. Morse, Philip M. and K. Uno Ingard Theoretical Acoustics, New York: McGraw-Hill Book Co., 1968.

24. Myers, J., C. Holm, and R. McAllister, Handbook of Ocean and Underwater Engineering, New York: McGraw-Hill Publishing Company, 1969.

25. Nussbaum, Allen, Electromagnetic Theory for Engineers and Scientists, Englewood Cliffs, N.J.: Prentice-Hall, Inc., 1965.

26. Reitz, John R. and Frederick J. Milford, Foundations of Electromagnetic Theory, Reading, Mass: Addison-Wesley Publishing Co., 1967.

27. Seyer, F.A. and A.B. Metzner, "Turbulence Phenomena in Drag Reducing Systems," Tehnical Report AD-696207, Office of Naval Research, 1969.

28. Sverdrup, H.U., Martin W. Johnson, and Richard H. Felming, The Oceans: Their Physics, Chemistry, and General Biology, Englewood Cliffs, N.J.: Prentice-Hall, Inc., 1942.

29. Uhlig, Herbert H., The Corrosion Handbook, New York: John Wiley and Sons, Inc., 1948.

APPENDICIES

The total Ohmic resistance of the electrolyte can be computed using the method of images. It is assumed that the two cylindrical electrodes are immersed in a conducting medium having lateral dimensions which are small compared to the separation distance of the electrodes. It is further assumed that the change per unit length ($\pm\lambda$) of the conductors is uniform. This assumption is not valid for the entire length of the conductor, however for small lengths of the conductor the variation with length is negligible. Since the resistance of the medium is a function of its electrical capacitance, and the capacitance at any point is determined by the local charge, the assumption is therefore applicable.

Beginning with Laplace's equation:

$$\nabla^2 U = o$$

For a given set of boundary conditions the solution is unique. If a solution $U(r,\theta,\phi)$ is obtained by any technique, and if all the boundary conditions are satisfied, then the solution is complete.

The potential difference between q and q', an imaginary charge, is given in cylindrical coordinates by

$$u(r,\theta,\phi) = \frac{q}{4\pi\epsilon_o r_1} + \frac{q'}{4\pi\epsilon_o r_2}$$

$$= \frac{1}{4\pi\epsilon_o}\left[\frac{q}{(r^2+d^2-2rd\cos\theta)^{1/2}} + \frac{q'}{(r^2+b^2-2rb\cos\theta)^{1/2}}\right]$$

Hence, for $r = a$, $u(a,\theta,\phi) = 0$ for all θ and ϕ. Thus, the radical terms must be proportional, or

$$b = \frac{a^2}{d}$$

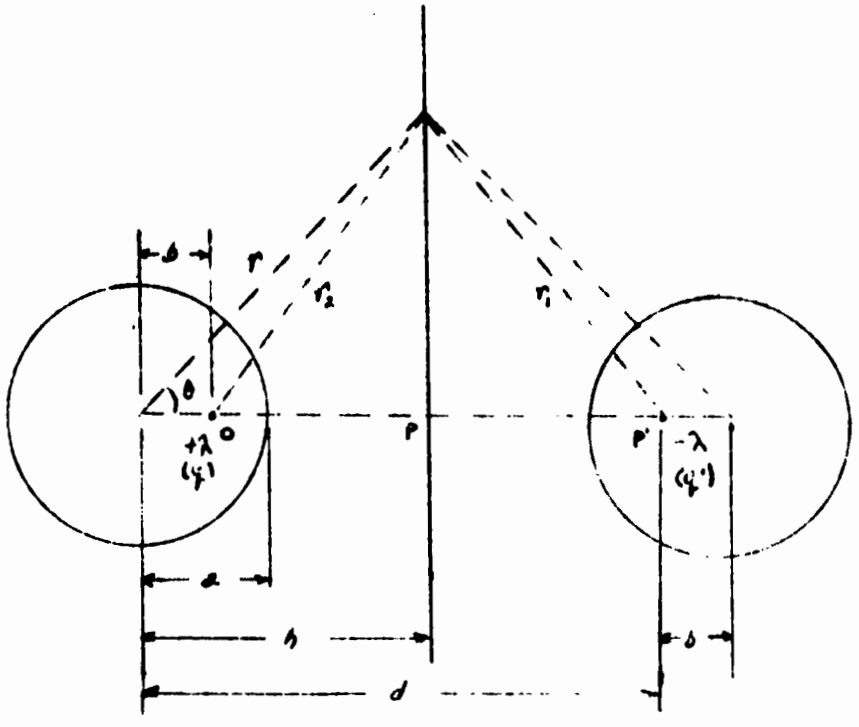

The capacitance of the pair of conductors is given by

$$\frac{Q}{V} = C = \frac{\lambda L}{V}$$

In terms of V,

$$V = \frac{\lambda L}{C}$$

$$= -\frac{\lambda}{2\pi\epsilon_o} (\ln r_1 - \ln r_2)$$

$$V = -\frac{\lambda}{2\pi\epsilon_o} (\ln r_1/r_2)$$

where ϵ_o is the permittivity of free space

(8.85×10^{-12} farad/meter).

Since $r_2 = d - \frac{a^2}{d} - r_1$

$$V = +\frac{\lambda}{2\pi\epsilon_o} \left(\ln \frac{d^2 - a^2 r_1 d}{r_1 d}\right)$$

The potential difference between o and p is

$$V_{op} = V_{(r=a-a^2/d)} - V_{(r=h-a^2/d)}$$

$$= \frac{\lambda}{2\pi\epsilon_o} \left\{\ln\left[\frac{d^2 - a^2 - d(a - a^2/d)}{d(a-a^2/d)}\right] - \ln\left[\frac{d^2 - a^2 - d(h-a^2/d)}{d(h-a^2/d)}\right]\right\}$$

$$V_{op} = \frac{\lambda}{2\pi\epsilon_o} \ln\left[\frac{hd - a^2}{a(d-h)}\right]$$

Recalling that $d = 2h - a^2/d$

$$d^2 - 2hd + a^2 = 0$$

$$d = h \pm \sqrt{h^2 - a^2}$$

Substituting this value for d

$$V_{op} = \frac{\lambda}{2\pi\epsilon_o} \ln\left[\frac{h^2+h(h^2-a^2)^{1/2}-a^2}{a(h^2-a^2)^{1/2}}\right]$$

$$= \frac{\lambda}{2\pi\epsilon_o} \ln\left[\frac{h}{a}+\frac{(h^2-a^2)}{a}\right]$$

$$V_{op} = \frac{\lambda}{2\pi\epsilon_o} \cosh^{-1}\left(\frac{h}{a}\right)$$

The potential difference between o and p' is $2V_{op}$, hence

$$\Delta u = \frac{\lambda}{\pi\epsilon_o} \cosh^{-1}\left(\frac{h}{a}\right)$$

The electric field intensity between the conductors is obtained from the equation

$$\vec{E} = -\nabla u$$

so that considering the x-direction only

$$E_x = -\frac{\partial u}{\partial x}$$

Since $\frac{\lambda}{2\pi\epsilon_o} = \frac{\Delta u}{2\cosh^{-1}(h/a)}$ and letting $r = (x^2+y^2)^{1/2}$

(where $x = 2h - \frac{a^2}{d} = d$)

$$E_x = -\frac{\Delta u}{2\cosh^{-1}(h/a)}\left[\frac{d(d^2+y^2)^{-1/2}2d}{d^2-a^2-d(d^2+y^2)^{1/2}}+\frac{(d^2+y^2)^{-1/2}2d}{(d^2+y^2)^{1/2}}\right]$$

The equation of continuity for the current through the surfaces of an arbitrarily-shaped surface area of macroscopic size is given by

$$I = \oint_S \vec{J} \cdot d\vec{n}\, da$$

Where $\vec{J}$ is the current density. Also, Ohm's Law can be written

$$\vec{J} = \frac{\vec{E}}{\rho}$$

ρ = restivity

Letting $ds = Ldy$, where L is the immersed electrode length

$$I = \frac{1}{\rho} \int_{-\infty}^{\infty} E dy$$

Substituting

$$I = \frac{\Delta u L d}{\rho \cosh^{-1}(h/a)} \int_{\infty}^{\infty} \left[\frac{d(d^2+y^2)^{-1/2}}{d^2-a^2-d(d^2+y^2)^{1/2}} + \frac{1}{(d^2+y^2)}\right] dy$$

Integrating this expression yields

$$I = \frac{\Delta u L \pi}{\rho \cosh^{-1}(h/a)}$$

Letting $s = 2h$, which is separation distance and $D = 2a$, where D is the electrode diameter, the total ohmic resistance is

$$R = \frac{\Delta u}{I} = \frac{\rho \cosh^{-1}(S/D)}{L\pi}$$

ILOOP

```
100 DIM V(9000)
110 DIM I(9000)
120 PRINT "INPUT ANODE AND CATHODE RESISTIVITY (MICRO-OHMS-CM)"
130 INPUT P1,P2
140 PRINT "INPUT OXIDATION-REDUCTION POTENTIAL"
150 INPUT E
160 PRINT "INPUT VALUES OF J0 AND ALPHA FOR ANODE AND CATHODE"
170 INPUT J8,A1,J9,A2
180 LET C1=LOG(J8)
190 LET C2=LOG(J9)
200 PRINT "INPUT MINIMUM AND LIMITING CURRENT DENSITY (AMPS/CM^2)"
210 INPUT J1,J2
220 PRINT "INPUT ELECTROLYTE RESISTIVITY (OHMS-CM)"
230 INPUT P3
240 PRINT "INPUT ELECTRODE DIAMETER (MILS) AND SEPARATION (CM)"
250 INPUT D,B
260 LET D=D*2.54/1000
270 PRINT "INPUT AVERAGE IMMERSED ELECTRODE LENGTH (CM)"
280 INPUT L
290 LET S=3.1416*L*D
300 PRINT "INPUT AVERAGE RECIPROCAL ELECTRODE LENGTH (1/CM)"
310 INPUT L1
320 LET L1=1/L1
330 PRINT "INPUT NUMBER OF DELTA-X DIVISIONS AND CONVERGENCE CRITERIA"
340 INPUT N,G
350 PRINT "INPUT NUMBER OF ELECTRODE PAIRS"
360 INPUT M
370 PRINT
380 PRINT
390 PRINT
400 LET R1=P1*L/(3.1416*(D/2)^2)*1E-6
410 LET R2=P2*L/(3.1416*(D/2)^2)*1E-6
420 LET R1=R1/N
430 LET R2=R2/N
440 LET R3=P3*LOG(B/D+SQR(B^2/D^2-1))/(3.1416*L1)
450 LET R3=R3*N
460 LET K=N
470 LET I(K)=J1*S
480 LET J=J1
490 LET Q=I(K)
500 LET U=0.0591*((LOG(J)-C1)/A1+(LOG(J)-C2)/A2)
510 LET V(K)=I(K)*R3+E+U
520 LET V(K-1)=V(K)+I(K)*(R1+R2)
530 LET Z=0.0591*((LOG((Q+I(K))/S)-C1)/A1+(LOG((Q+I(K))/S)-C2)/A2)
540 IF ABS(Q-(V(K-1)-E-Z)/R3)<G THEN 570
550 LET Q=Q+Q/1000
560 GO TO 530
570 LET I(K-1)=I(K)+Q
580 LET K=K-1
590 IF K=0 THEN 660
```

ILOOP (CONTINUED)

```
600 LET J=I(K)/S
610 IF J<J2 THEN 500
620 IF Q1<>0 THEN 500
630 LET Q1=1
640 LET Z1=(N-K)/N
650 GO TO 500
660 LET V0=V(1)+I(1)*(R1+R2)
670 PRINT "APPLIED VOLTAGE IS ";V0;" VOLTS"
680 PRINT "CURRENT FOR ONE PAIR IS ";I(1);" AMPS"
690 PRINT "TOTAL CURRENT IS ";I(1)*M;" AMPS"
700 PRINT
710 IF Q1<>1 THEN 740
720 PRINT "CURRENT DENSITY EXCEEDS LIMITING VALUE AT X= ";Z1
730 PRINT
740 PRINT "TOTAL RESISTANCE OF ONE ELECTRODE PAIR IS ";V0/I(1);" OHMS"
750 PRINT "TOTAL CIRCUIT RESISTANCE IS ";V0/(I(1)*M);" OHMS"
760 PRINT
770 PRINT
780 PRINT
790 PRINT "X","I(X) (AMPS)","J(X)","[DI/DX]","D/D0"
800 PRINT
810 LET K=1
820 PRINT " 0",I(1),I(1)/S,
830 LET B=(I(K)-I(K+1))/(L/N)
840 LET B=B0
850 PRINT B0," 1.0"
860 LET K=K+1
870 IF INT(K/(N/10))<>K/(N/10) THEN 910
880 LET B=(I(K)-I(K+1))/(L/N)
890 PRINT (N-K)/N,I(K),I(K)/S,B,B/B0
900 GO TO 860
910 IF K=N THEN 930
920 GO TO 860
930 LET B=I(K)/(L/N)
940 PRINT " 1.0",I(K),I(K)/S,B,B/B0
950 END
```

78<

LIST OF VARIABLES

P1,P2 - Anode and Cathode Resistivity
P3 - Electrolyte Resistivity
E - Oxidation-Reduction Potential
J8,J9- Values of J0 for Tafel Equation
A1,A2- Values of Alpha for Tafel Equation
C1,C2- Constants associated with Log(J0)
J1- Minimum Current Density
J2- Limiting Current Density
D- Electrode Diameter
B- Electrode Separation Distance
L- Average Electrode Length
L1- Average Reciprocal Electrode Length
S- Electrode Surface Area
N- Number of Delta-X Divisions
G- Convergence Criteria
M- Number of Electrode Pairs
R1,R2- Total and Differential Electrode Resistances
R3- Total and Differential Electrolyte Resistances
K- Index Variable
I(K)- Local Current
J- Local Current Density
Q- Local Current in Parallel Resistor
U- Tafel Overpotential
V(K)- Local Potential Difference
Z- Incremented Tafel Overpotential
Q1- Control Variable
Z1- Location of First Excess of Current Density over Limiting Value
V0- Applied Voltage
I(1)- Total Cell Current
B- Change in Current with respect to distance
B0- Initial Value of B

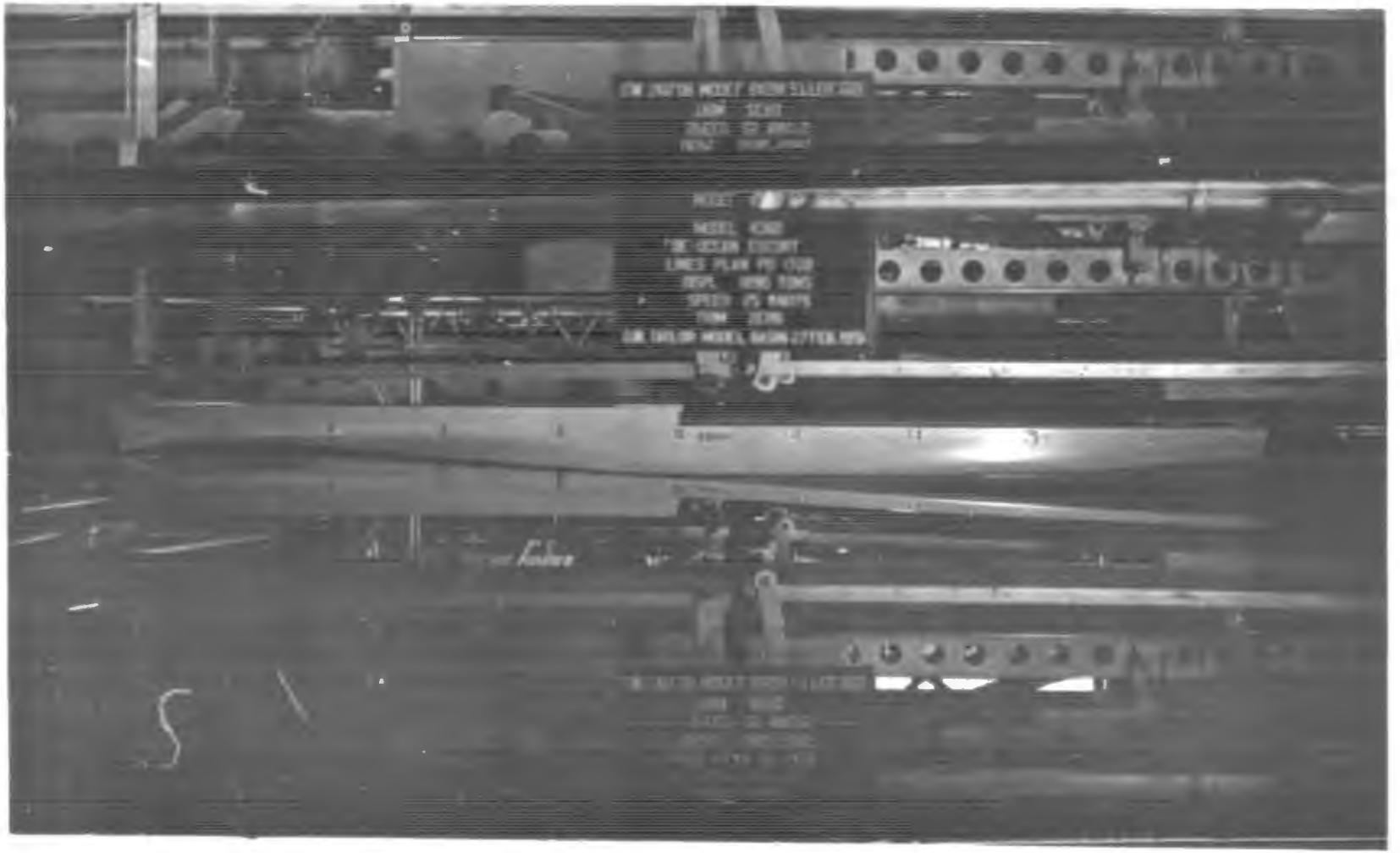

Photograph showing bare-hull wave profile (18'2" model)
(Courtesy of Naval Ship Research and Development Center)

Photographs showing wave profiles (1.4 knots and 5.0 knots) 5' model

C3

Photographs showing 5' model towed at 2.2 knots with electrodes attached (0 amps and 1.0 amps)

D1

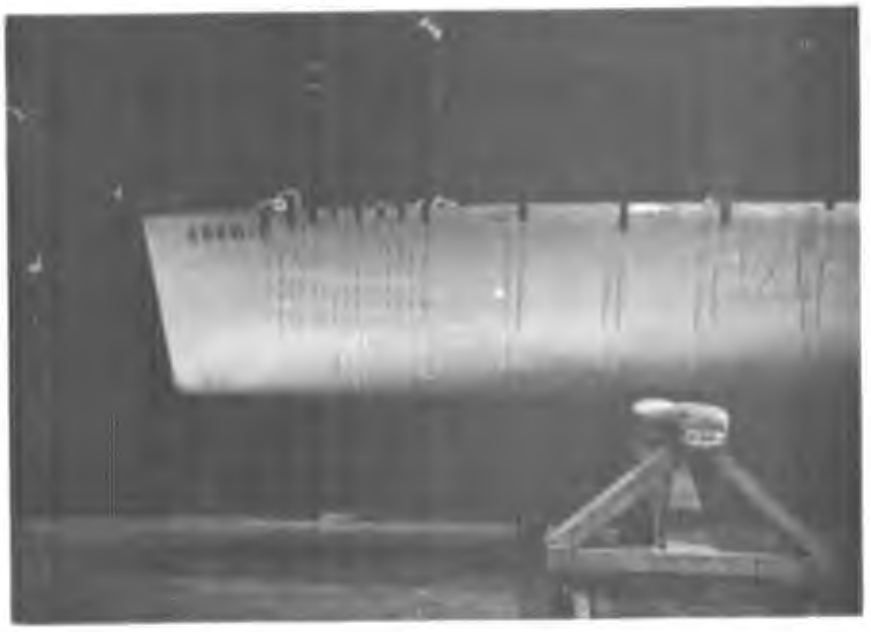

Photographs showing electrode configuration tested on 18'2" model. Only the copper electrodes are visible.

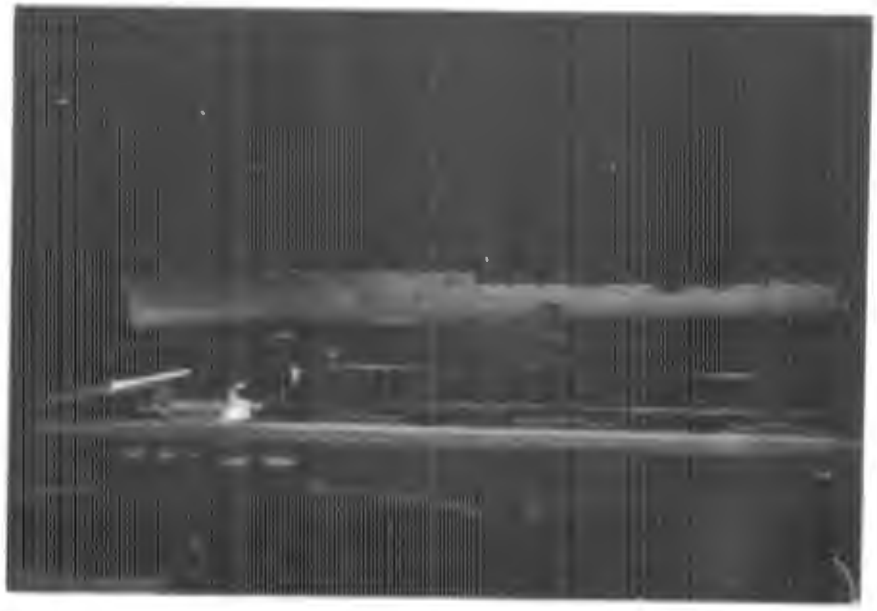

Photograph showing electrode configuration tested on 18'2" model.